Physical basis for long-distance communication along meiotic chromosomes

Kyle R. Fowler[a,1,2], Randy W. Hyppa[a,1], Gareth A. Cromie[a,3], and Gerald R. Smith[a,4]

[a]Division of Basic Sciences, Fred Hutchinson Cancer Research Center, Seattle, WA 98109

Edited by Thomas D. Petes, Duke University Medical Center, Durham, NC, and approved August 16, 2018 (received for review February 5, 2018)

Viable gamete formation requires segregation of homologous chromosomes connected, in most species, by cross-overs. DNA double-strand break (DSB) formation and the resulting cross-overs are regulated at multiple levels to prevent overabundance along chromosomes. Meiotic cells coordinate these events between distant sites, but the physical basis of long-distance chromosomal communication has been unknown. We show that DSB hotspots up to ∼200 kb (∼35 cM) apart form clusters via hotspot-binding proteins Rec25 and Rec27 in fission yeast. Clustering coincides with hotspot competition and interference over similar distances. Without Tel1 (an ATM tumor-suppressor homolog), DSB and crossover interference become negative, reflecting coordinated action along a chromosome. These results indicate that DSB hotspots within a limited chromosomal region and bound by their protein determinants form a clustered structure that, via Tel1, allows only one DSB per region. Such a "roulette" process within clusters explains the observed pattern of crossover interference in fission yeast. Key structural and regulatory components of clusters are phylogenetically conserved, suggesting conservation of this vital regulation. Based on these observations, we propose a model and discuss variations in which clustering and competition between DSB sites leads to DSB interference and in turn produces crossover interference.

meiosis | crossover interference | DNA break interference | DSB hotspot clustering | *S. pombe*

During meiosis, the diploid chromosome set in somatic cells is reduced to a haploid set to form gametes for sexual reproduction. Successful chromosome segregation requires that the two parental homologs segregate from each other at the first meiotic division, in sharp contrast to mitotic divisions, in which sister chromatids segregate from each other. Meiotic homolog segregation requires their mutual recognition. In most eukaryotic species this entails formation, by homologous genetic recombination, of a physical connection in regions of extensive DNA sequence identity. In addition to these connections (called "cross-overs"), cohesion between sister chromatids, by cohesin protein complexes, is required to form tension between homologs, which facilitates the onset of proper homolog segregation (1). A crossover too near another may leave too little cohesion to effectively hold the homologs together and thereby provide the necessary tension. Consequently, most species have evolved a mechanism of communication along chromosomes to prevent cross-overs from occurring too near each other. This phenomenon, called "crossover interference," was discovered over 100 y ago (2), but its mechanism has remained elusive.

Homologous recombination, including crossover formation, occurs at high frequency during meiosis and is initiated by the formation of DNA double-strand breaks (DSBs) by Spo11 (or its homolog) and several essential partner proteins (Fig. 1*A*) (3). Repair of a DSB by interaction with the homolog can lead to a crossover, measured genetically by the formation of reciprocal recombinants between homologs appropriately marked. A hierarchical combination of factors shapes the genome-wide topography of meiotic DSBs. Like cross-overs, DSBs are controlled in both frequency and distribution along chromosomes (3). Short chromosomal intervals with especially high frequency of DSBs (called "DSB hotspots") are separated by cold regions with relatively low DSB frequency. In the fission yeast *Schizosaccharomyces pombe*, studied here, DSB hotspots occur roughly 30–50 kb apart, and nearly all are bound with high specificity by three small, putatively coiled-coil proteins, Rec25, Rec27, and Mug20, which are also required for the formation of nearly all DSBs at nearly all hotspots (4). These hotspot-determinant proteins appear to form a complex with Rec10, which is required for all meiotic DSB formation and recombination genome-wide. These four proteins, with other chromosomal components, form linear elements (LinEs) related to the synaptonemal complex (SC) of other species (4, 5). Thus, LinE proteins dictate the formation of both DSBs at hotspots and chromosomal structures. We report here that these functions are related and have a common purpose—the physical coordination of DSB formation to prevent their overabundance along chromosomes.

We find that DSB hotspots bound by LinE proteins form 3D clusters that encompass chromosomal regions of ∼200 kb. We also observe competition between DSB hotspot sites and interference between DSBs occurring on the same molecule, with both these effects extending over similar physical distances as hotspot clustering. We propose a model in which limiting the number of breaks within a cluster produces both DSB interference and hotspot competition; we present evidence that this limitation is imposed by the DNA damage-response protein kinase Tel1 (an

Significance

Formation of viable sex cells, such as eggs and sperm in humans, occurs during a special type of cell division (meiosis), in which parental chromosomes (homologs) must separate from each other. In most species this process requires a physical connection between homologs; these connections, called "cross-overs," arise from DNA breaks, which occur at high frequency at special sites called "hotspots." Successful meiosis requires that DNA double-strand breaks (DSBs) and the resulting cross-overs be carefully controlled. We describe here a physical mechanism for control of DSBs between distant hotspots via the 3D clustering of hotspots bound by their determinant proteins. Based on these results, we propose a physical mechanism for crossover interference, which was discovered over 100 y ago but whose mechanism has remained elusive.

Author contributions: K.R.F., R.W.H., G.A.C., and G.R.S. designed research, performed research, contributed new reagents/analytic tools, analyzed data, and wrote the paper.

The authors declare no conflict of interest.

This article is a PNAS Direct Submission.

Data deposition: The data in this paper have been deposited in the Gene Expression Omnibus (GEO) database, https://www.ncbi.nlm.nih.gov/geo (accession no. GSE119921).

[1]K.R.F. and R.W.H. contributed equally to this work.

[2]Present address: Department of Microbiology and Immunology, University of California, San Francisco, CA 94143.

[3]Present address: Pacific Northwest Diabetes Research Institute, Seattle, WA 98122.

[4]To whom correspondence should be addressed. Email: gsmith@fredhutch.org.

This article contains supporting information online at www.pnas.org/lookup/suppl/doi:10.1073/pnas.1801920115/-/DCSupplemental.

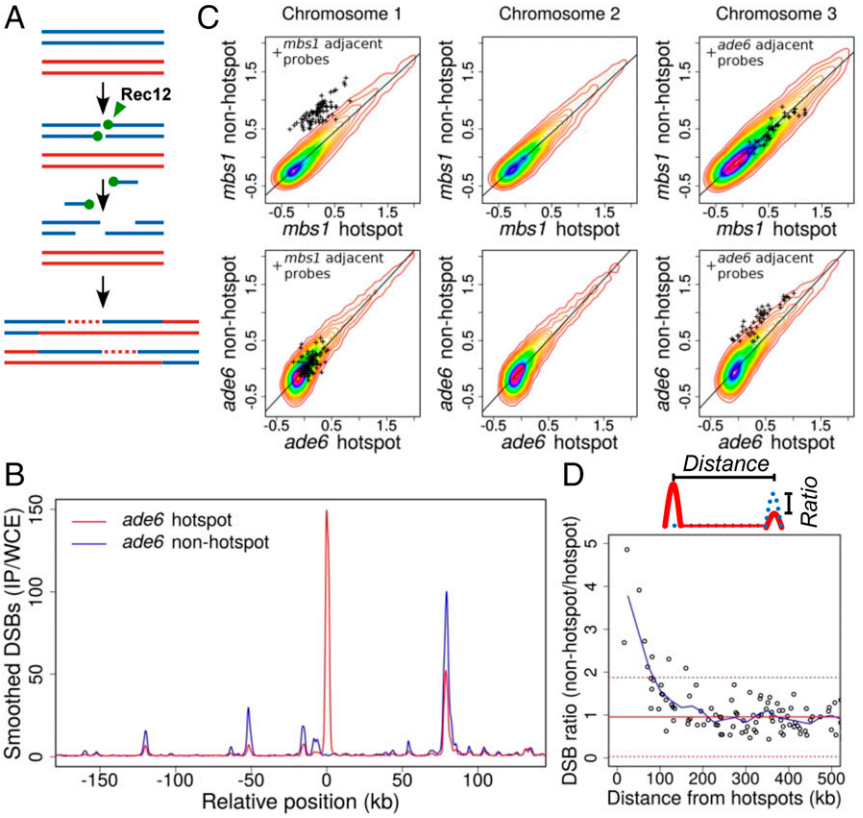

Fig. 1. DSB hotspots compete with each other over ~200-kb regions. (*A*) Rec12 (Spo11 homolog; green ball) forms DSBs, remains covalently linked to 5′ ends, and is removed by an endonuclease to expose 3′ single-stranded tails (30, 58). Tails invade homologous DNA to form joint DNA molecules, resolved to form cross-overs as shown or non–cross-overs. Each line is ssDNA, blue and red from each parent; dashed lines indicate newly synthesized DNA. (*B*) DSBs are reduced at hotspots within ~100 kb of the Rec25, Rec27-dependent *ade6-3049* hotspot (4, 10, 24). Shown is DSB frequency, measured by ChIP-chip of Rec12-DNA covalent complexes, on part of Chr 3 with (*ade6-3049*; red line) or without (*ade6-3057*; blue line) a hotspot. (*C*) DSB frequency is increased only on the chromosome with hotspot alteration. (*Upper*) Natural hotspot *mbs1* on Chr 1 (*mbs1*$^+$ vs. *mbs1-20* deletion). (*Lower*) *ade6* hotspot on Chr 3 (*ade6-3049* vs. *ade6-3057*). (*SI Appendix*, Fig. S1) (11). Individual points (+) are microarray values at other hotspots ≤50 kb of each side of the compared hotspot. Heat maps (densest in magenta) indicate densities of other points. Scales, $\log_{10}$. (*D*) Competition extends ~100 kb on each side of a hotspot. Hotspot peaks surrounding *mbs1* or *ade6-3049* were integrated in the presence or absence of *mbs1* or *ade6-3049*; each hotspot's DSB ratio was plotted against its distance from *mbs1* or *ade6-3049*. Values >1 indicate more breakage in the absence of each hotspot. Data were averaged (blue line) using a 50-kb sliding window in 25-kb steps. Median ratio is 0.95 (solid red line); dashed red lines indicate median ± two SD.

ATM homolog, a tumor suppressor) (6–8). Because DSBs give rise to cross-overs, this proposed model leads to a mechanism for crossover interference and provides a means of communicating the DNA state between distant points regardless of chromosome physical size.

Results

Hotspots for Meiotic DSB Formation Compete with Each Other over ~200-kb Regions. To assess communication between DSB hotspots along a chromosome, we first determined the effect of adding or deleting a hotspot on the frequency of DSBs at nearby hotspots. We assayed genome-wide the immediate product of DSB formation—DNA covalently linked to Rec12 (Spo11 homolog) (Fig. 1*A*)—by immunoprecipitation of Rec12-DNA complexes and hybridization to tiling microarrays (9). By comparing two strains with and without the single base pair mutation *ade6-3049*, which creates a strong DSB hotspot (10), we observed that DSBs at hotspots flanking *ade6-3049* were reduced, compared with the nonhotspot control, as far as ~100 kb to each side (Fig. 1*B*). Conversely, when we deleted the natural hotspot *mbs1* on a different chromosome (11), DSBs became readily detectable at minor hotspots, previously barely visible, up to ~100 kb on each side of *mbs1* (*SI Appendix*, Fig. S1). In both experiments DSBs far from the manipulated hotspot, or on the other two chromosomes, arose at nearly the same frequency (Fig. 1*C*). This effect, called "DSB competition," is locally limited to an ~200-kb region encompassing the break site (Fig. 1*D*). This interval size is similar to the average distance between DSBs [~60 DSBs across the 12,600-kb genome (12)]. This outcome is consistent with only one DSB being made per ~200-kb region (within a "cluster" as discussed below). DSB competition has also been reported in budding yeast but over somewhat shorter distances (up to ~70 kb) (13–17). In both yeasts, however, these distances correspond to ~25–35 cM, somewhat less than the genetic distance (50 cM) resulting from one crossover (*Discussion*).

In Fission Yeast, DSB Hotspots Compete in *cis* but Not in *trans*. To test if this form of communication (hotspot competition) occurs along only one of the two parental homologs (in *cis*) or also extends between homologs (in *trans*), we tested the effect of having two nearby hotspots on the same or on different homologs (Fig. 2). Our first test used two previously studied hotspots, *ade6-3049* and an inserted copy of *ura4*$^+$ about 15 kb away (called "*ura4A*") (18, 19). When alone and heterozygous, *ura4A* gave 3.6% DSBs. When *ade6-3049* was added only in *trans*, this DSB level was not significantly changed (3.1% DSBs; $P > 0.07$ by unpaired *t* test). However, when *ade6-3049* was added only in *cis,* the DSB level of *ura4A* was significantly reduced by about half, to 1.65% DSBs ($P < 0.0005$ by unpaired *t* test). Therefore, *ade6-3049* competed against *ura4A* significantly more in *cis* than in *trans* (1.65% vs. 3.1% DSBs at *ura4A*; $P < 0.0001$ by unpaired *t* test) and may, in fact, not compete at all in *trans*. Furthermore, each individual hotspot showed about twice the DSB level when homozygous as when heterozygous, suggesting that there is little if any self-competition in *trans*. Additional comparisons of the data show that the stronger hotspot, *ade6-3049*, was not significantly competed by the weaker hotspot, *ura4A*. In a second assay of DSB competition, using two artificial hotspots about 45 kb apart, we also found competition in *cis* but not in *trans*. In this case the slightly weaker hotspot competed against the slightly stronger one (*SI Appendix*, Fig. S2). In *Saccharomyces cerevisiae* DSB competition occurs both along and between the two homologs (13–17, 20). In *S. pombe* we conclude that DSB competition occurs along only one homolog.

Interference of DSB Formation Along One DNA Molecule Is also Limited to ~200-kb Regions. The analysis above showed that DSB hotspots compete with one another on the same homolog but not between homologs. To assess the ability of a DSB to interfere with DSB formation at another site on a given chromatid (i.e., along one DNA molecule), we assayed the frequency

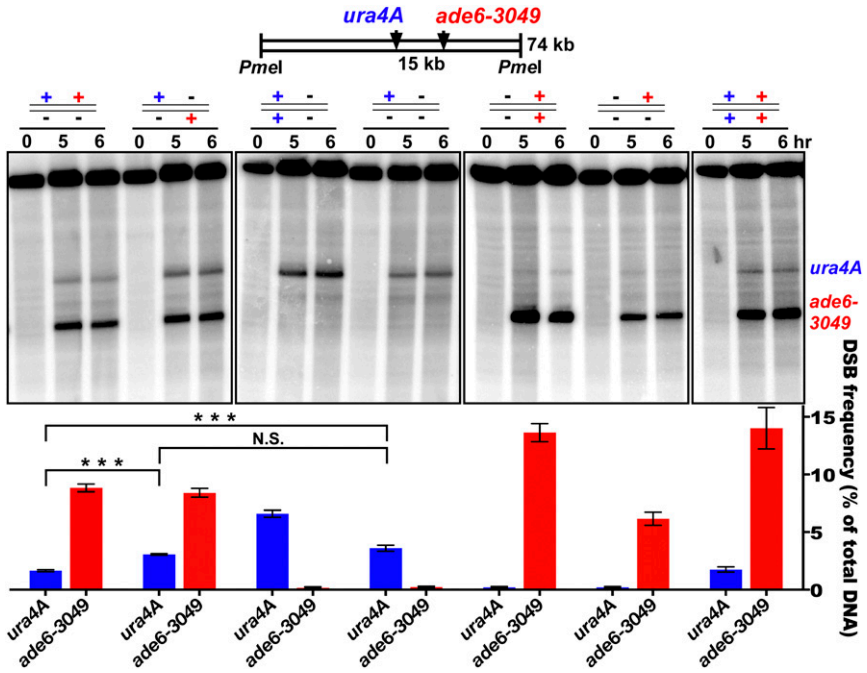

Fig. 2. DSB competition acts along a homolog (in *cis*) but not between homologs (in *trans*). *ura4A* (blue) and *ade6-3049* (red) DSB hotspots on Chr 3 were on the same (in *cis*; leftmost lane set) or different (in *trans*, second lane set) parental homologs. +, hotspot present; −, hotspot absent. DSBs were assayed at the indicated times after induction of meiosis in *rad50S* [wild-type DSB distribution (59)]. Data (mean ± SEM; $n = 3$ or 4) show the percent of DNA broken at the indicated hotspot (assay probe at the right end of the PmeI fragment). The fourth lane set from the left (no *ade6* hotspot) shows that the *ura4A* hotspot is reduced by *ade6-3049* in *cis* (first lane set; ***$P < 0.0005$ by unpaired *t* test) but not in *trans* [second lane set; $P > 0.07$ by unpaired *t* test; N.S. (not significant)]. The first two lane sets show that *ade6-3049* reduces the *ura4* hotspot more in *cis* than in *trans* (***$P < 0.0001$ by unpaired *t* test). See *SI Appendix*, Table S3 for individual data and *SI Appendix*, Fig. S2 for additional competitive pairs.

of DNA molecules broken at each of two nearby hotspots. DSB frequency was assayed by Southern blot hybridization of DNA extracted from meiotic cells, cut by an appropriate restriction enzyme, and separated by gel electrophoresis. A radioactive probe homologous to DNA located between the two chosen hotspots, about 15 kb apart, allowed concurrent assay (i.e., on the same Southern blot hybridization) of the frequency of DNA broken at one or the other or both hotspots (Fig. 3*A*). We found that doubly broken DNA was three to five times less frequent than expected from breakage at the two sites independently (i.e., the product of the frequency of breakage at each individual site) (Fig. 3 *B* and *C* and *SI Appendix*, Fig. S3). Thus, breakage at one site interferes with breakage at the other on the same DNA molecule. We observed DSB interference under multiple conditions for inducing meiosis (21, 22) and between several additional hotspot pairs on different chromosomes, ranging from ∼15–125 kb apart (Fig. 3*D* and *SI Appendix*, Figs. S3–S5). The extent of DSB interference, like that of DSB competition, decreased with distance, however, and became markedly less at ∼200 kb (Figs. 1 and 3 and *SI Appendix*, Figs. S3–S5 and Table S1).

DSB interference and DSB competition may reflect the same phenomenon (*Discussion*), but their assays are different: Interference assays one DNA molecule encompassing two hotspots, whereas DSB competition assays all four chromatids (DNA molecules) at a site distant from the one genetically altered. They are also conceptually distinct: Interference indicates that breakage at two nearby hotspots on the same DNA molecule occurs less frequently than expected from independent breakage at the two sites. Competition indicates that the overall frequency of breakage across a region is dependent on the presence or absence of another nearby hotspot. Because DSB interference and competition have similar distance dependencies and could plausibly stem from the same phenomenon, we infer that they do; but because their assays are different and could be mechanistically different, we refer to them with different terms.

Tel1 DNA Damage-Response Protein Kinase Controls DSB and Crossover Interference. In a mutant (*tel1Δ*) lacking the Tel1 protein kinase (ATM homolog) important for the DNA damage response (6), DSB interference was eliminated (Fig. 3), as reported in budding yeast (8). In fact, in fission yeast we observed more doubly broken DNA than expected from independent breakage, indicating negative DSB interference. [Interference (I) is quantitatively defined as 1 − CoC, where CoC (coefficient of coincidence) = $R_D/R_1 \cdot R_2$; R_D is the frequency of double events, and R_1 and R_2 are the frequencies of the individual events. Thus, observing more double events than expected from independence yields negative interference.] Negative interference was observed in *tel1Δ* mutants over distances from ∼15 kb to 125 kb but not significantly at 250 kb (Fig. 3 *C* and *D* and *SI Appendix*, Figs. S3–S5 and Table S1). These results support the notion that protein phosphorylation by Tel1 kinase is involved in controlling communication along meiotic chromosomes (*Discussion*) (8).

Furthermore, double cross-overs in the two adjacent genetic intervals *ura2–leu2–lys7*, each with a strong DSB hotspot ∼15 kb apart (4, 12), were also observed at a higher-than-expected frequency in the *tel1Δ* mutant ($I = -0.85 \pm 0.072$, $n = 16$; $P < 0.0001$ by one-sample *t* test) (Table 1 and *SI Appendix*, Table S2). Consistent with this result, we observed negative DSB interference between these two DSB hotspots in the *tel1Δ* mutant (*SI Appendix*, Fig. S5). This negative crossover interference shows that cross-overs in fission yeast can be formed within a limited chromosomal region in a concerted fashion in *tel1Δ*. In *tel1*$^+$ we observed a low but significant level of positive crossover interference ($I = 0.28 \pm 0.033$, $n = 17$; $P < 0.0001$ by one-sample *t* test) (Table 1 and *SI Appendix*, Table S2); a previous report also found low but significant positive interference (0.33 and 0.29) in

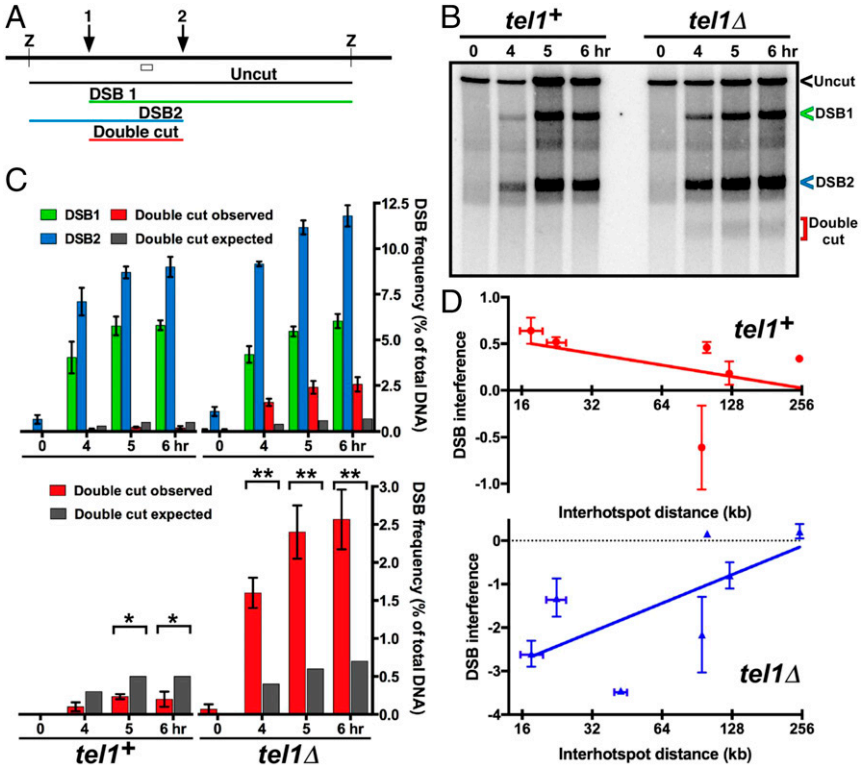

Fig. 3. Interference of DSB formation at nearby hotspots depends on Tel1 DNA damage-response protein kinase. (*A*) Scheme for assaying DSB frequency at either one or both hotspots (1 and 2) by Southern blot hybridization of DNA cut by restriction enzyme Z; the open box indicates the probe position. (*B*) DSB interference between two hotspots about 15 kb apart near the left end of Chr 2. (*C*) The observed doubly broken fragment (red bars) is less frequent than expected from independent breakage at the two hotspots (dark gray bars) in wild type but is more frequent than expected in *tel1Δ*. See *SI Appendix*, Figs. S3–S5 and Table S1 for additional data. (*D*) DSB interference is positive in *tel1*$^+$ but negative in *tel1Δ* mutants. Error bars indicate SEM or range (*SI Appendix*, Table S1).

two intervals tested (23). Thus, cross-overs appear not to be formed in a simple random (independent) fashion as previously supposed in this yeast (*Discussion*) (23). As expected, no significant crossover interference, either positive or negative, was observed between intervals on different chromosomes in *tel1*$^+$ ($I = 0.02 \pm 0.066$, $n = 16$; $P = 0.99$ by one-sample t test) (*SI Appendix*, Table S2*B*) or in *tel1Δ* ($I = -0.10 \pm 0.059$, $n = 16$; $P = 0.06$ by one-sample t test) (*SI Appendix*, Table S2*C*). This outcome bolsters the significance of the observed positive and negative interference between adjacent chromosomal intervals in *tel1*$^+$ and *tel1Δ*, respectively. These results further show that recombination sites along a chromosome, but not between different chromosomes, indeed communicate regionally in individual meiotic cells, as also demonstrated by DSB competition and DSB interference in wild-type populations (Figs. 1–3, Table 1, and *SI Appendix*, Figs. S1–S5 and Tables S1–S3). Thus, in *tel1* mutants both DSBs and cross-overs manifest negative interference, a result of coordinated action along the chromosome.

Hotspots Physically Cluster over ∼200-kb Chromosomal Regions via DSB Hotspot-Determining Proteins. DSB competition and DSB interference indicate that breakage at one hotspot reduces or eliminates breakage at another hotspot over a limited chromosomal region. We hypothesized that these effects result from physical interaction of hotspots within this region. To test this hypothesis, we assessed the close physical association of hotspots bound by LinE proteins, which bind hotspots with high specificity, are required for the formation of most DSBs at nearly all hotspots, and form nuclear foci visible by light microscopy of live cells (Fig. 4*A*) (4, 24). We assayed the relative proximity (clustering) of hotspot DNA using a modification of the chromosome-conformation-capture (3C) technique, related to chromatin interaction analysis by paired-end tag sequencing (ChIA-PET) (25, 26),

Table 1. Cross-overs show strong negative interference in *tel1* mutants

Strain	Crossover interval 1, %*	Crossover interval 2, %†	Double crossover observed, %	Double crossover expected, %	Interference‡
tel1$^+$	**3.76** ± 0.26	**17.5** ± 2.1	**0.49** ± 0.081	**0.67** ± 0.11	**0.26** ± 0.051§
tel1Δ	**3.02** ± 0.14	**8.0** ± 0.54	**0.47** ± 0.048	**0.245** ± 0.025	**−0.90** ± 0.048

In five (*tel1*$^+$) and eight (*tel1Δ*) independent crosses, crossover recombination was assayed in the *ura2 – leu2 – lys7* intervals (1 and 2, respectively), each of which contains a strong Rec25, Rec27-bound DSB hotspot (4, 12). Data are mean ± SEM. See *SI Appendix*, Table S2*A* for individual data and *SI Appendix*, Table S2 *B* and *C* for additional data. Bold face indicates mean values.

*Interval 1 is *ura2 – leu2* on Chr 1.

†Interval 2 is *leu2 – lys7* on Chr 1.

‡Interference = 1 – (double crossover observed/double crossover expected).

§The near-zero values for most intervals reported by Munz (23) may not be significantly different from the value reported here, since many fewer recombinants were reported by Munz than were observed here. Two intervals showed weak but significant positive interference (I = 0.33 and 0.29).

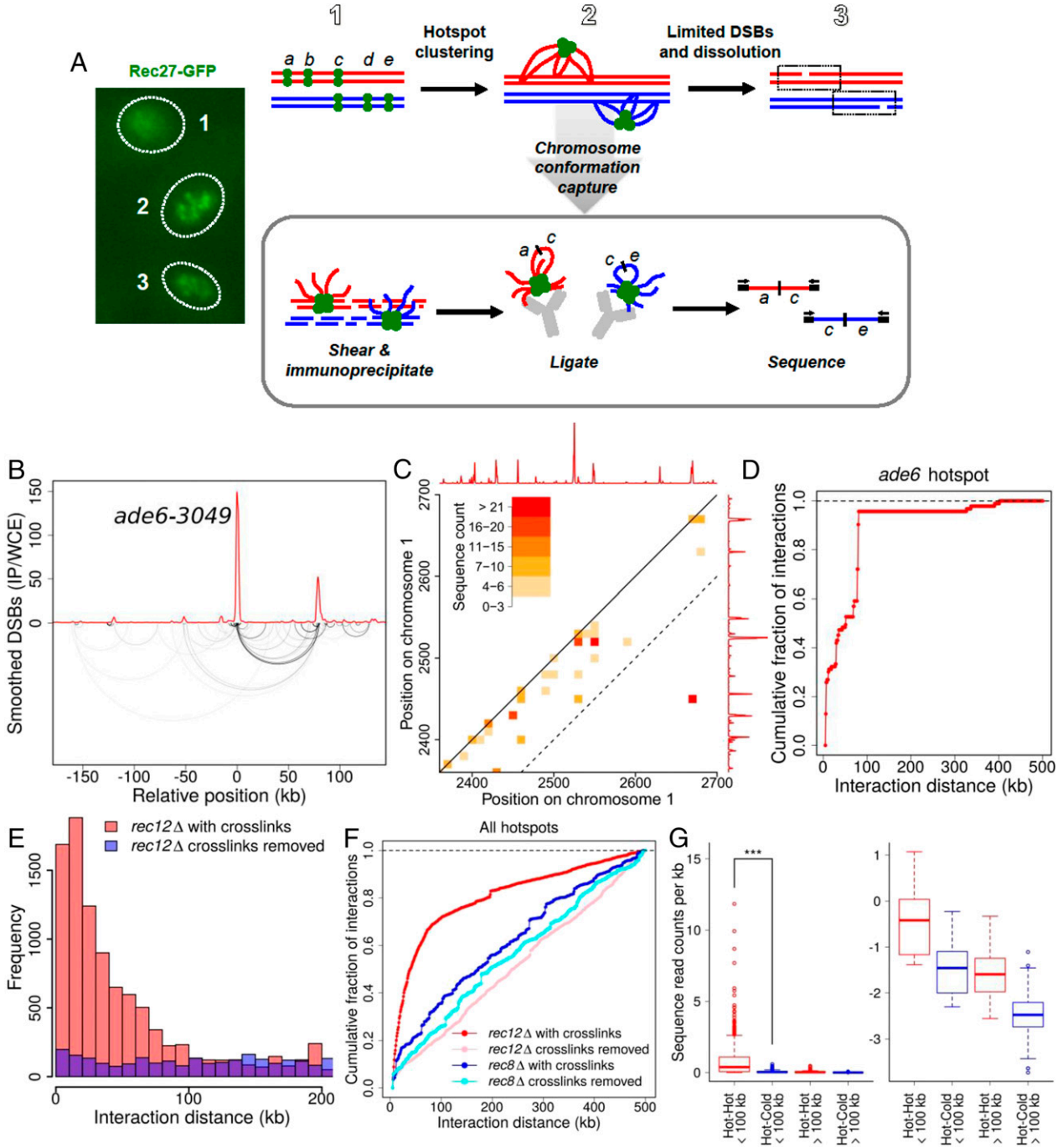

Fig. 4. Physical clustering of DSB hotspots is limited to an ~200-kb chromosomal region. (*A*) Scheme for determining clustering of DSB hotspots bound by LinE proteins, such as Rec27-GFP, which form a limited number of foci (or clusters of foci) in meiotic nuclei (*Left*) (31), perhaps corresponding to the steps in the *Upper* row. DNA within each cluster is cross-linked to a tagged LinE protein and analyzed as indicated in the box (see text). (*B*) Analysis of DNA bound by Rec27-GFP, which binds DSB hotspots with high specificity (4), shows preferential ligation of the *ade6-3049* hotspot DNA to another hotspot ~80 kb away (lower arcs; darker lines indicate greater frequency). Ligated sequences were omitted if neither end mapped to a hotspot. The red line indicates DSB frequency relative to genome median, determined by microarray hybridization (4). See also *SI Appendix*, Fig. S7. (*C*) Standard contact heat-map of ligations (hot–hot and hot–cold) in the 2,350–2,700 kb region of Chr 1. DSB frequency relative to the genome median (red line, on a linear scale) is from ref. 12. The dashed line indicates positions 100 kb apart on the chromosome; note that most of the intense interactions are within this limit, with the exception of ligations between two hotspots about 250 kb apart. See also *SI Appendix*, Figs. S8–S10. (*D*) Summation of all ligations between the *ade6-3049* hotspot and DNA within 500 kb of each side. (*E*) Distance between pairs of sites ligated among all genomic hotspots with chromatin cross-links maintained until after ligation (red bars) or with cross-links removed just before ligation (purple bars; blue where these values are greater than those with maintained cross-links). (*F*) Summation of ligations between all genomic hotspots with chromatin cross-links maintained until after ligation (red line) or with cross-links removed just before ligation (pink line). Preferential ligations between nearby hotspots are much less frequent and extend greater distances in the absence of the Rec8 cohesin subunit with (dark blue line) or without (light blue line) maintenance of chromatin cross-links (see also *SI Appendix*, Fig. S13). (*G*, *Left*) Ligations between hotspots <100 kb apart are more frequent than those >100 kb apart (***$P < 0.001$ by unpaired *t* test). (*Right*) The same data are shown on a $\log_{10}$ scale for clarity of low levels. Data are the number of ligations per kilobase; mean values (thick horizontal bars) are flanked by the 25th and 75th percentiles (boxes) and 95th percentiles (whiskers). See *SI Appendix*, Fig. S6*D* for additional data with Rec25 and with another tag for immunoprecipitation and *SI Appendix*, Figs. S6–S13 for additional data.

which relies on DNA ligation frequency as a proxy for distance. We cross-linked the DNA and closely bound proteins in meiotic cells, extracted and mechanically sheared the chromatin, and immunoprecipitated the hotspot-determinant proteins Rec25 or Rec27 (fused to appropriate epitope tags) to enrich for hotspot interactions involving these proteins. We ligated the closely apposed DNA ends and used paired-end sequencing to determine the genomic locations of the ends ligated together (*SI Appendix*, Fig. S6).

This methodology differed in two important ways from typical 3C procedures, which likely would have failed to detect the relatively infrequent physical interactions between hotspots anticipated from our analyses above. First, after cross-linking the chromatin, we randomly sheared it by sonication rather than digesting it with a site-specific nuclease (27). This modification disrupted the compacted nuclear organization, which would have produced the abundant, short-range interactions observed in standard 3C analyses. Second, as noted above, we immunoprecipitated a hotspot-binding protein (Rec27 or Rec25) to enrich for specific protein–DNA complexes of interest (DSB hotspots). These two modifications reduced the more abundant, widespread interactions in standard 3C analyses, which likely would have obscured the rare hotspot-specific interactions studied here (see below). The ends of the sheared, immunoprecipitated DNA were then ligated and prepared for paired-end deep sequence analysis; the sequences in each pair were independently mapped to the fission yeast genome (28). Genome-wide analyses showed that many readily ligated ends came from two hotspot sites that were up to ∼100 kb apart on the linear genome sequence but must have been close in 3D space in the nucleus at the time of cross-linking. Similar procedures were used in *S. pombe* for different chromosomal proteins but, as expected, with markedly different results (26, 29) (see below).

Preferential ligation between nearby hotspot DNAs is exemplified by the *ade6-3049* hotspot bound by Rec27-GFP (4). Of the ends ligated to *ade6-3049*, ∼40% came from another Rec27-bound hotspot ∼80 kb away, shown by the arcs connecting two interacting, well-separated chromosomal sites in Fig. 4*B*. Similar results were observed at several hotspot pairs on a different chromosome (*SI Appendix*, Fig. S7*A*). Preferential hotspot–hotspot interaction is also shown by a conventional "contact map" (Fig. 4*C* and *SI Appendix*, Figs. S7–S10) in which the most intense interactions are at points (squares) connecting two hotspots. Summation of all of the DNA ends ligated to the *ade6-3049* hotspot showed a rapid accumulation over the first 100 kb followed by a much slower accumulation of ligated ends farther apart (Fig. 4*D*). Averaging all 603 hotspots (i.e., including even very minor ones) in the genome (12) refined the pattern and demonstrated preferential ligation of hotspots to sites <100 kb away (Fig. 4 *E* and *F*). Ligations were most frequent between hotspots 10–20 kb apart and became less frequent with increasing interhotspot distance (Fig. 4*E*). Nearly all cross-link–dependent ligations were between DSB hotspots 100 kb apart or less on the given chromosome (Fig. 4*E* and *SI Appendix*, Fig. S11). This feature is also evident in the contact map: Most of the intense interactions occur within ∼100 kb of the diagonal representing the chromosome (Fig. 4*C* and *SI Appendix*, Figs. S7–S10). Most of the longer-range (>100 kb), less frequent ligations likely result from random association of DNA ends across the genome. As expected, they accumulate at constant, low rate with linear chromosomal distance, as do ligations observed when Rec27-DNA cross-links were removed just before ligation (Fig. 4*F*). Also as expected, ligations between sites on different chromosomes were much less frequent, per kilobase, than ligations within 100 kb on the same chromosome (*SI Appendix*, Fig. S11).

To determine if this proximity-dependent association is hotspot-specific, we partitioned the genome into DSB-hot and DSB-cold regions and calculated the frequency of ligation events per kilobase. Ligation of hotspot DNA to other nearby hotspot DNA (i.e., <100 kb away) was on average ∼14 times more frequent than ligation to either proximal cold-region DNA or distant hotspot DNA (>100 kb away) and was >100 times more frequent than ligation to distant cold-region DNA ($P < 0.001$ for each comparison) (Fig. 4*G* and *SI Appendix*, Fig. S11*A*). Note that ∼77% of the chromosomal DNA is in DSB-cold regions by the cutoff used here (12); cross-linking and ligation of random neighboring DNA would predict only 0.23 times as many ligations of a hotspot to another hotspot as to any chromosomal point at random. Thus, in the nuclear 3D space hotspot DNA is much closer to other hotspot DNA nearby on the linear genome than to other DNA, as shown by the standard contact maps in Fig. 4*C* and *SI Appendix*, Figs. S7–S10 and S12*A*. As expected, LinE-bound DNA ligations are discontinuous (site-specific) across a genomic region, whereas standard Hi-C and ChIA-PET ligations are continuous (monotonically decreasing with distance) across the same genomic region (*SI Appendix*, Fig. S12) (26, 29). As deduced from the data analysis above, most pairs of ligated chromosomal sites occur <100 kb apart, and the most highly enriched pairs are between hotspots <100 kb apart (Fig. 4 and *SI Appendix*, Fig. S11). We note, however, that there are rare exceptions to this general rule: A few DSB hotspots are not fully dependent on Rec27 (4), some ligations occurred between hotspots >100 kb apart, and some hotspots were ligated at only low frequency (Fig. 4*C* and *SI Appendix*, Figs. S7–S10). We take the more general, abundant ligations preferentially between DSB hotspots <100 kb apart (Fig. 4*G*) as evidence for clustering of these sites by the hotspot-determinant protein Rec27.

Note that our results differ markedly from those obtained by Hi-C or the analysis of cohesin and condensin proteins in *S. pombe* involving similar procedures of chromatin cross-linking and sonication followed by immunoprecipitation and DNA ligation (Fig. 4 and *SI Appendix*, Fig. S12) (26, 29). These two proteins preferentially bind to and organize certain chromosomal intervals of up to ∼80 kb (cohesin) or ∼300 kb (condensin). Each protein appears to bind a fixed preferred site at the edge of the interval and one of many other sites within the adjacent interval, suggesting chromatin loops with one fixed and one variable chromosomal point. Alternatively, all the sites in an interval may be in a compact structure that allows ligation between any two points within the interval. By contrast, our results show ligations between well-separated, isolated points—LinE-bound DSB hotspots. (The similarity of these interval sizes and those of clusters may reflect related factors influencing their formation.)

Our hotspot clustering analyses were done in the absence of DSB formation (i.e., in the absence of Rec12) (30), indicating that the interactions occur without, and therefore likely before, DSB formation and are not due to DNA repair processes. This result is expected because binding of Rec27 to hotspots is independent of Rec12 (4), as is focus formation by other LinE proteins Rec10 and Mug20 (31, 32). Similar results were obtained using a different epitope tag (FLAG) and a different antibody for immunoprecipitation of Rec27 and when Rec25 immunoprecipitates were analyzed (*SI Appendix*, Fig. S6*D*), indicating the robustness of these results. The meiosis-specific cohesin subunit Rec8 is required for Rec27 to form most foci, bind to nearly all hotspots, and form DSBs at them (4). As expected, preferential ligations were much rarer in the absence of Rec8 than in the absence of Rec12 and were considerably farther apart on average (Fig. 4*F* and *SI Appendix*, Fig. S13). This outcome is expected, because these remaining (Rec8-independent, Rec27-bound) DSB hotspots are located on average >400 kb from each other (4). Focus formation of LinE proteins Rec10, Rec25, and Rec27 appeared normal in *tel1Δ* mutants (*SI Appendix*, Fig. S14), suggesting that clusters form independently of Tel1.

In summary, we observed close physical interactions between DSB sites over limited chromosomal distances with two LinE

proteins, independent of the tag used but largely dependent on Rec8 and the maintenance of cross-links before ligation.

Discussion

Our results presented here show that DSB hotspot competition and interference extend along chromosomes for distances (~200 kb) very similar to that of hotspot clustering (~200 kb). This observation and the coordinate effects of genetic mutations on these features strongly suggest that clusters provide the physical basis for DSB competition and DSB interference. In other words, DSB hotspots communicate along chromosomes via the formation of physical interactions between the DSB hotspots that are bound by their determinant proteins. We discuss the implications of our results for regulating the formation not only of DSBs but also the cross-overs arising from them.

Evidence for Hotspot–Hotspot Interactions Forming Localized Clusters of LinE-Bound Hotspots. Our data here (Fig. 4 and *SI Appendix*, Figs. S6–S13) indicate that DSB hotspots over a limited chromosomal region are located sufficiently close to each other to be cross-linked by formaldehyde, to remain associated during sonication and immunoprecipitation, and to allow ligation of the DNA ends produced by sonication and "polishing." This standard procedure is an established method for determining the association of distant chromosomal sites in 3D space (25). We employed these standard procedures, with modifications that have been previously used (26, 29), to show that meiotic DSB hotspots within a limited chromosomal region (~200 kb) are more frequently associated with each other than are hotspots farther apart or on another chromosome and that within that limited region a hotspot is associated much more frequently with other hotspot DNA than with cold-region (nonhotspot) DNA. Detecting the enhanced hotspot–hotspot interactions (which form clusters) depends on cross-linking and thus these interactions are not random; the spatial and hotspot-specific preferences also show that these interactions are neither random nor due to normal chromosome compaction. Furthermore, these interactions require the Rec8 cohesin subunit, which is required for loading of the LinE proteins Rec25 and Rec27 (31), the proteins we analyzed for clustering. Collectively, these observations show that LinE-bound DSB hotspots form clusters over a limited chromosomal region.

Relations Between DSB Hotspot Clustering, DSB Competition, and DSB Interference. The genetic and physical data presented here indicate that DSB hotspot clusters are closely related to DSB competition and DSB interference. (As noted above, competition and interference may reflect the same phenomenon but are conceptually distinct and are observed by distinct assays.) First, all three phenomena occur over approximately the same distance, ~200 kb (Figs. 1, 3, and 4). This is also the average distance between DSBs (12). Second, the LinE proteins Rec25 and Rec27 bind DSB hotspots with high specificity and are required for DSB formation at nearly all these hotspots (4). These proteins form readily visible, colocalizing foci in meiotic cells (4, 31) and, by the type of 3C analysis used here (related to ChIA-PET) (Fig. 4), form clusters of hotspot sites located across chromosomal regions of ~200 kb. Third, genetic removal of the meiosis-specific cohesin subunit Rec8 greatly reduces binding of Rec27 to hotspots, formation of microscopic foci, formation of DSBs at hotspots, and formation of hotspot clusters (Fig. 4) (4, 31). Fourth, the *ade6-3049* single base pair mutation creates a strong binding site for LinE proteins and a strong LinE-dependent DSB hotspot; it also imparts localized cluster formation, DSB competition, and DSB interference (Figs. 1–4) (4, 10, 24). Fifth, the Tel1 protein kinase imparts both DSB interference and crossover interference; in its absence, both become negative (Fig. 3, Table 1, and *SI Appendix*, Figs. S1–S5). These results are consistent with a causal connection between these two phenomena. Collectively, these observations demonstrate that these features arise from a common source, the clustering of LinE-bound DSB hotspots and the limiting of DSB formation within these clusters. We discuss below the mechanistic implications of hotspot clustering.

Molecular Basis of DSB Hotspot Competition and DSB Interference Within a Hotspot Cluster. Limiting the number of DSBs that can occur within a cluster can explain both hotspot competition between chromatids and DSB interference between hotspots on a single DNA molecule. Hotspot sites within a cluster compete for the limited number of DSBs that can be formed in a cluster. Adding a new strong hotspot, such as *ade6-3049*, will reduce the overall frequency of breakage at nearby existing hotspots. Similarly, limiting the number of DSBs within a cluster means that a break at one site will reduce the probability of a second break at another nearby site on the same DNA molecule within the cluster, resulting in DSB interference.

How might DSB formation be limited within hotspot clusters? We propose that formation of the first DSB within a cluster physically alters the proteins, DNA, or both within a cluster such that a second DSB is formed at reduced frequency or perhaps not at all, in which case one cluster produces one DSB. This proposal is consistent with ~60 DSBs per meiosis (12) being distributed by competition and interference across the 12.6-Mb fission yeast genome and with previous conclusions of a limit, at a given locus, of only one DSB per homolog pair in many meiotic cells in budding yeast (20, 33, 34). For example, modification of one or more proteins in the cluster may change the protein's activity and thereby prevent further DSB formation. Specifically, when the first DSB is formed, the Tel1 protein kinase may be activated and then phosphorylate, and thereby inactivate, a component of the DSB-forming complex [Rec12 and its half-dozen essential partner proteins (35)]. This feature readily accounts for Tel1 and its kinase activity being required for DSB interference and suppression of nearby cross-overs in fission yeast (Fig. 3, Table 1, *SI Appendix*, Figs. S2–S5 and Table S2), for full levels of DSB and crossover interference in budding yeast (8, 34), and for strong restriction of DSB formation in mice (7). We note that Tel1 is not required, however, for focus formation by the LinE proteins Rec25, Rec27, or Rec10 (*SI Appendix*, Fig. S14). This result suggests that Tel1 acts to control DSB formation after hotspots are clustered by the LinE proteins. Binding and clustering of the DSB machinery in the absence of Tel1 may also explain strong negative interference of both DSBs and cross-overs in the absence of Tel1 (Fig. 3, Table 1, and *SI Appendix*, Figs. S2–S5 and Tables S1 and S2). The close proximity of the uncontrolled DSB-promoting factors may result in frequent breakage at multiple sites in a cluster and thus the formation of multiple, closely spaced cross-overs.

An alternative (or additional) mechanism to limit DSB formation is a limiting component, e.g., the active-site protein Rec12, within each cluster such that only one DSB can be formed. Finally, the conformation of the DSB-forming complex may change and prevent further DSB formation, as is the case for the recombination hotspot-activator RecBCD enzyme of *Escherichia coli* (36).

DSB Interference as a Basis of Crossover Interference. Closely related to DSB interference is crossover interference, the occurrence of closely spaced double cross-overs less frequently than expected under independence. Given that DSBs are the precursors to cross-overs, DSB interference would be expected to give rise to crossover interference. Therefore, based on our results here, we propose the following physical basis for meiotic crossover interference and the model in Fig. 5. This model may apply to some but not all species, for there are clearly variations

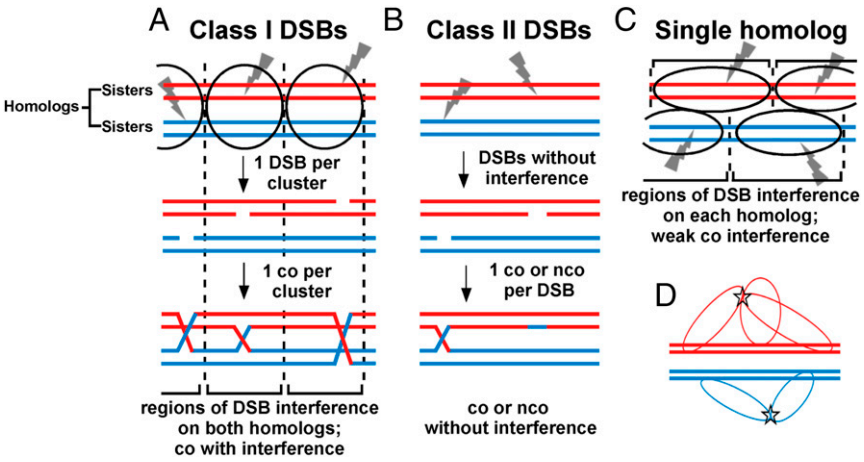

Fig. 5. Model for crossover interference based on DSB interference among clustered DSB hotspots. Each horizontal line is one sister chromatid (dsDNA molecule), red for one parental homolog (pair of sister chromatids) and blue for the other. Ovals indicate clusters, within which one DSB (gray lightning bolt) occurs. (*A*) In species with complete interference, clusters of activated DSB hotspots on both homologs form in a limited chromosomal region; only one DSB (class I) is made in each cluster. Consequently, no more than one crossover is made in that region, resulting in crossover interference. In a population of cells, clusters are distributed more or less randomly; interference is thus complete in short genetic intervals but becomes less in longer genetic intervals and is negligible in genetic intervals equal to or greater than that resulting from one crossover (50 cM). (*B*) In some species, class II DSBs are also formed but are not cluster-controlled and consequently do not manifest interference. Crossover interference is incomplete but is greater if class I DSBs outnumber class II DSBs. (*C*) In some species, such as fission yeast, clusters form between activated DSB hotspot sites on one homolog, not two. Consequently, DSBs (class I) manifest interference (on one DNA molecule), but cross-overs manifest only weak interference, since DSBs form independently on the two homologs (*Discussion*). (*D*) Flexible chromatin loops enable very distant DSB hotspots bound by their activating protein determinants to form a cluster. DSB hotspots on chromatin loops could extend from the chromosomal axis (central thick lines, each a dsDNA molecule or sister chromatid) and thereby allow activated DSB hotspots to form a cluster (star), even though they might be at the extremities of the chromosome. Clusters might form over both homologs (as in *A*) or over only one homolog (as in *C*).

in the mechanism and control of meiotic recombination among species. Furthermore, in addition to DSB interference there may be other mechanisms of crossover interference such as those proposed by others (37–41). In species with strong crossover interference, we propose that potential sites of DSB formation form clusters encompassing both homologs, and a single DSB is made in each cluster (Fig. 5*A*). (Note that in any given cell these potential sites are only the sites in a chromosomal region bound by hotspot-determinant proteins; they are not all the sites in a chromosomal region at which DSBs are made in the population of cells.) Consequently, no more than one crossover can arise in the clustered region, which would encompass a genetic distance of no more than 50 cM, the genetic distance resulting from one crossover. If clusters are more or less randomly distributed across the genome in a population, interference would be nearly complete at short genetic distances (a few centimorgans) but would disappear as distances approach 50 cM. At short distances, both genetic intervals for crossover assays would be in the same cluster, whereas at longer distances they would be in, or extend over, two or more clusters, which act independently. This is the outcome observed in some species (41), which we propose have clusters and DSBs regulated as in Fig. 5*A*. Most eukaryotes have extensive heterochromatic regions devoid of DSBs around their centromeres (42). We suppose that DSB hotspot clusters do not form in or across such pericentric regions, thereby explaining why crossover interference does not occur across the centromere in some cases.

Variation of crossover interference in other species can be accounted for by two classes of DSBs and by clusters encompassing both homologs or only one (Fig. 5 *B* and *C*). Two classes of cross-overs have been identified previously in various species (34, 43), those manifesting interference (class I) and those manifesting weak or no interference (class II). We propose that these crossover classes correspond to two classes of DSBs, as follows. The first DSB made in a cluster (here called "class I") is unique in that it prevents the formation of further DSBs of its type in that cluster. Any additional DSBs (here called "class II") made subsequently are repaired to either noninterfering crossovers or non–cross-overs. Class II DSBs may arise either within clusters (after class I DSBs are formed) or outside clusters; the latter case seems simpler and accounts for DSBs formed independently of hotspot determinants (4, 12). In species with incomplete crossover interference, both class I and class II crossovers occur. The designation of the first DSB as class I, and thus the designation of an interfering crossover, could be made either before or at the time of that DSB formation; both possibilities are compatible with the general scheme proposed here. We further note that if DSB formation is weakened, e.g., by alteration of the DSB-forming protein Spo11 (44), fewer class II DSBs are made after the first (class I) DSB is made. Thus, the frequency of interfering cross-overs, the major class, is maintained despite fewer total DSBs being made and at the expense of fewer non–cross-overs from class II DSBs. This feature, called "crossover homeostasis" (44), is thereby accounted for, as is the concurrent loss of crossover interference and crossover homeostasis in certain mutants (45).

In the two species reported to have weak or no crossover interference (*S. pombe* and the fungus *Aspergillus*) (Table 1 and *SI Appendix*, Table S2) (23), we propose that most or all DSBs are interfering (class I) but occur in clusters encompassing only one homolog (Fig. 5*C*) rather than both homologs, as in species shown in Fig. 5*A* (33, 34). This feature may reflect incomplete synaptonemal complex formation between homologs in *S. pombe* and *Aspergillus* (5); the SC has long been associated with crossover interference (46, 47). Although *S. pombe* LinE proteins form structures similar to the lateral elements of the SC, *S. pombe* has no obvious orthologs of the SC central elements which connect homologs in other species. The apparent absence of central element components is consistent with the proposal that *S. pombe* makes clusters encompassing only one homolog. Cluster formation on only one homolog also accounts for DSB competition acting along a homolog (in *cis*) but not between homologs (in *trans*) in *S. pombe* (Fig. 2 and *SI Appendix*, Fig. S2). If clusters on the two homologs are independently distributed,

there would be DSB interference, as assayed on single DNA molecules, but only weak crossover interference, as observed (Fig. 3, Table 1, *SI Appendix*, Figs. S3–S5 and Tables S1 and S2). Because DSBs could arise independently on each homolog even in a short interval, double cross-overs would be observed. However, the absence of two DSBs on each individual homolog (i.e., only one DSB arising per pair of sister chromatids) would reduce the frequency of total DSBs in a cluster-size interval relative to their frequency under complete independence; consequently, there would be weak crossover interference only over short intervals, as observed (Table 1 and *SI Appendix*, Table S2). Thus, this proposal solves the seeming paradox of strong (positive) DSB interference without strong (positive) crossover interference in fission yeast. It also explains the paradoxical observation of strong negative crossover interference (I = –0.85) in the absence of Tel1 (Table 1 and *SI Appendix*, Table S2). The concerted formation of both DSBs and cross-overs in *tel1* mutants indicates that *S. pombe* has, like species manifesting (positive) crossover interference, the basic mechanism of communication over a long distance along a chromosome.

To our knowledge, only one publication has discussed DSB interference as the basis for crossover interference. Berchowitz and Copenhaver (48) discussed DSB competition and crossover interference extending over about 70 kb in *S. cerevisiae* (16, 49), but they dismissed the possibility that DSB interference might explain crossover interference over much larger (megabase) regions, as observed in most multicellular species. However, the flexibility of loops in chromatin provides a basis for the long-distance communication between sites bound by DSB hotspot determinants (i.e., not over entire, continuous regions) along chromosomes discussed above. We propose that the potential sites at which DSBs could be made occur on loops emanating from the chromosomal axis and that the protein-bound sites form a cluster (Fig. 5*D*). These potential sites are limited to the few bound to their protein determinants in a particular cell; they are not all the sites in the included chromosomal region at which DSBs are made in the population. In *S. pombe*, only sites bound by LinE proteins in a particular cell would form a cluster. Note that the chromosomal regions between these sites are not proposed to be in the cluster; the majority of the chromosome can remain in the extended linear form of the axis or synaptonemal complex. In a 20-μm-diameter nucleus, such as that of a human oocyte (50), two loops of about 60 kb would allow sites at the ends of a 100-Mb chromosome to cluster in this way. (60 kb is for B-form DNA; nucleosome-containing DNA would require about 200 kb, but each of these DNA lengths is a small fraction of the entire chromosome and would likely be invisible by ordinary microscopy.) Thus, we see no difficulty in DSB site clustering, and consequently DSB interference, being the basis for crossover interference even for large chromosomes.

Clusters have been previously discussed in connection with crossover interference. Stahl (51) proposed that "recombination nodules," thought to be protein complexes that promote meiotic recombination, might be swept into "piles" (clusters) to impose crossover interference. Stahl et al. (52) similarly proposed that "crossover intermediates," presumably joint DNA molecules, or "attempts," presumably crossover and non–crossover events combined, might form finite clusters in an interval. To our knowledge, 3D clustering of DSB sites has not been previously proposed.

1D clusters of DSBs along a chromosome, like birds clustered along a telephone wire, have been observed and discussed extensively (e.g., refs. 8 and 34). These clusters are physically and conceptually distinct from the 3D clusters of DSB hotspots discussed here, (Fig. 5). Garcia et al. (8, 53) proposed that DSB hotspots along several clustered chromatin loops are physically separate but subject to Tel1-independent DSB competition and that DSB hotspots along one loop are separate but subject to Tel1-dependent DSB interference. Anderson et al. (34) proposed a model for crossover interference incorporating 1D clusters of DSBs regulated by the synaptonemal initiation complex (SIC) and Tel1. In this model, DSBs are made independent of either factor; an SIC binds a DSB and prevents, in a Tel1-dependent manner, further nearby DSB formation, resulting in Tel1-dependent crossover interference. The fundamental basis of crossover interference in this model is SIC positioning (by an unspecified mechanism, but see below), whereas in our model it is 3D clustering of DSB hotspots (by LinE complex formation) and limitation of LinE-dependent DSBs.

Comparison of DSB Hotspot Clusters and Beam-Film Meshworks as the Basis of Long-Distance Chromosomal Communication. The conservation of communication along meiotic chromosomes invites a comparison of two models proposed to account for such communication—the "beam-film" model for crossover interference (37) and the clustering model for DSB and crossover interference presented here (Fig. 5). The beam-film model posits that mechanical stress on the chromosomes, partially dependent on topoisomerase II (45), builds up until a crossover is formed, locally relieving the stress and thereby discouraging a second, nearby crossover. Chromosomes are proposed to fold in three dimensions and form a "meshwork" of contacts, also unspecified, between distant sites within which stress is built up and relieved (45). Our clustering model and data reported here provide a structural and mechanistic basis for several of these concepts, with clusters taking the place of meshworks. One significant difference between the two models, however, is the level at which interference operates. The beam-film model posits that stress is relieved by crossing over, not by DSB formation, and therefore interference applies to cross-overs but not to DSBs. In contrast, in our hotspot 3D clustering model (Fig. 5) interference applies to DSBs and therefore also to the cross-overs that result from them. Data from both *S. cerevisiae* (8) and our current study in *S. pombe* clearly demonstrate the existence of DSB interference, supporting the clustering model.

Materials and Methods

Materials. *S. pombe* strains are listed in *SI Appendix*, Table S4 with their genotypes, sources, and the figures or tables in which data from them are presented. Growth media were rich yeast extract liquid (YEL; Difco), yeast extract agar (YEA; Difco), appropriately supplemented Edinburgh minimal media (EMM2), pombe minimal glutamate (PMG), nitrogen base agar (NBA; Difco), sporulation agar (SPA), and malt extract agar (MEA; Difco) (54). Reagents for the preparation and analysis of DNA are as described in ref. 55. Oligonucleotides are listed in *SI Appendix*, Table S5. Meiotic chromatin was immunoprecipitated (4) using anti-GFP (Roche) or anti-FLAG (Invitrogen) antibodies. DNA ligations used T4 DNA ligase (New England Biolabs). Amplification of immunoprecipitated DNA was carried out using either a Sequenase version 2.0 DNA Sequencing Kit (Affymetrix) or a REPLI-g Single Cell Kit (Qiagen).

Analysis of Meiotic Recombination. Crosses were conducted on supplemented SPA and analyzed as described in ref. 54 and *SI Appendix*, Table S2.

Preparation and Analysis of Meiotic DNA. *S. pombe* cultures were grown and induced for meiosis as described (55, 56). For analysis of DSBs by Southern blot hybridization in Fig. 3 and *SI Appendix*, Figs. S3 and S4, DNA was extracted with phenol-chloroform from cells in liquid buffer (57) and analyzed as described (55). (Cells were not embedded in agarose plugs before DNA extraction to avoid diffusion and thus loss of the small doubly broken DNA fragments from the plugs.) For analysis of DSBs by Southern blot hybridization in Fig. 2 and *SI Appendix*, Figs. S2 and S5, cells were embedded in agarose, and DNA was extracted and analyzed as described (55). The genomic regions analyzed and the restriction enzymes used were as follows: in Fig. 2 and *SI Appendix*, Figs. S3 and S4, 1.26–1.34 Mb on chromosome (Chr) 3, cut with PmeI; in Fig. 3 and *SI Appendix*, Fig. S2, 0.94–0.99 Mb on Chr 2, cut with AvrII; in *SI Appendix*, Fig. S5*A*, 0.52–1.02 Mb on Chr 1, cut with NotI; *SI Appendix*, Fig. S5*B*, 4.08–5.08 Mb on Chr 1, cut with NotI; in *SI Appendix*, Fig. S5*C*,

3.03–4.53 Mb (right end) on Chr 2, cut with NotI; in *SI Appendix*, Fig. S5*D*, 2.72–3.60 Mb on Chr 1, cut with NotI.

Analysis of DNA Proximity by Chromosome-Conformation Capture. The analysis of DNA proximity by chromosome-conformation capture is described in the *SI Appendix*.

ACKNOWLEDGMENTS. We thank the Fred Hutchinson Cancer Research Center Shared Resources Group for expert DNA sequence analyses; Paul Russell for the *tel1::kanMX6* allele; Yoshinori Watanabe for the *cnp20::2FLAG-kanMX6* allele; José Ayte for the *pat1-as1* allele; Emily Higuchi for strains and information on DSB and crossover interference; Gabriel Cortez, Hannah Sue Hults, and Mai-Chi Nguyen for technical assistance; Sue Amundsen, Harmit Malik, Peter Kushner, Michael Lichten, Mridula Nambiar, Tom Petes, Rasi Subramaniam, Stephen Tapscott, Jeetu Thakur, and SaraH Zanders for comments on the manuscript; and Greg Copenhaver for discussions about crossover interference. This work was supported by NIH Grants R01 GM031693, R01 GM032194, and R35 GM118120 (to G.R.S.) and P30 CA015704 to the Fred Hutchinson Cancer Research Center. Data on DSB competition, DSB interference, and hotspot 3D clustering and a model for crossover interference based on these data were reported by G.R.S. at the 2011 European Molecular Biology Organization Conference on Meiosis and at subsequent annual meetings.

1. Petronczki M, Siomos MF, Nasmyth K (2003) Un ménage à quatre: The molecular biology of chromosome segregation in meiosis. *Cell* 112:423–440.
2. Sturtevant AH (1915) The behavior of the chromosomes as studied through linkage. *Z Indukt Abstamm Vererbungsl* 13:234–287.
3. Lam I, Keeney S (2014) Mechanism and regulation of meiotic recombination initiation. *Cold Spring Harb Perspect Biol* 7:a016634.
4. Fowler KR, Gutiérrez-Velasco S, Martín-Castellanos C, Smith GR (2013) Protein determinants of meiotic DNA break hot spots. *Mol Cell* 49:983–996.
5. Loidl J (2006) *S. pombe* linear elements: The modest cousins of synaptonemal complexes. *Chromosoma* 115:260–271.
6. Langerak P, Russell P (2011) Regulatory networks integrating cell cycle control with DNA damage checkpoints and double-strand break repair. *Philos Trans R Soc Lond B Biol Sci* 366:3562–3571.
7. Lange J, et al. (2011) ATM controls meiotic double-strand-break formation. *Nature* 479:237–240.
8. Garcia V, Gray S, Allison RM, Cooper TJ, Neale MJ (2015) Tel1(ATM)-mediated interference suppresses clustered meiotic double-strand-break formation. *Nature* 520:114–118.
9. Cromie GA, et al. (2007) A discrete class of intergenic DNA dictates meiotic DNA break hotspots in fission yeast. *PLoS Genet* 3:e141.
10. Steiner WW, Smith GR (2005) Optimizing the nucleotide sequence of a meiotic recombination hotspot in *Schizosaccharomyces pombe*. *Genetics* 169:1973–1983.
11. Cromie GA, Rubio CA, Hyppa RW, Smith GR (2005) A natural meiotic DNA break site in *Schizosaccharomyces pombe* is a hotspot of gene conversion, highly associated with crossing over. *Genetics* 169:595–605.
12. Fowler KR, Sasaki M, Milman N, Keeney S, Smith GR (2014) Evolutionarily diverse determinants of meiotic DNA break and recombination landscapes across the genome. *Genome Res* 24:1650–1664.
13. Jessop L, Allers T, Lichten M (2005) Infrequent co-conversion of markers flanking a meiotic recombination initiation site in *Saccharomyces cerevisiae*. *Genetics* 169:1353–1367.
14. Fan QQ, Xu F, White MA, Petes TD (1997) Competition between adjacent meiotic recombination hotspots in the yeast *Saccharomyces cerevisiae*. *Genetics* 145:661–670.
15. Robine N, et al. (2007) Genome-wide redistribution of meiotic double-strand breaks in *Saccharomyces cerevisiae*. *Mol Cell Biol* 27:1868–1880.
16. Wu TC, Lichten M (1995) Factors that affect the location and frequency of meiosis-induced double-strand breaks in *Saccharomyces cerevisiae*. *Genetics* 140:55–66.
17. Xu L, Kleckner N (1995) Sequence non-specific double-strand breaks and interhomolog interactions prior to double-strand break formation at a meiotic recombination hot spot in yeast. *EMBO J* 14:5115–5128.
18. Zahn-Zabal M, Lehmann E, Kohli J (1995) Hot spots of recombination in fission yeast: Inactivation of the *M26* hot spot by deletion of the *ade6* promoter and the novel hotspot *ura4-aim*. *Genetics* 140:469–478.
19. Baur M, et al. (2005) The meiotic recombination hot spot *ura4A* in *Schizosaccharomyces pombe*. *Genetics* 169:551–561.
20. Fukuda T, Kugou K, Sasanuma H, Shibata T, Ohta K (2008) Targeted induction of meiotic double-strand breaks reveals chromosomal domain-dependent regulation of Spo11 and interactions among potential sites of meiotic recombination. *Nucleic Acids Res* 36:984–997.
21. Guerra-Moreno A, Alves-Rodrigues I, Hidalgo E, Ayté J (2012) Chemical genetic induction of meiosis in *Schizosaccharomyces pombe*. *Cell Cycle* 11:1621–1625.
22. Iino Y, Yamamoto M (1985) Negative control for the initiation of meiosis in *Schizosaccharomyces pombe*. *Proc Natl Acad Sci USA* 82:2447–2451.
23. Munz P (1994) An analysis of interference in the fission yeast *Schizosaccharomyces pombe*. *Genetics* 137:701–707.
24. Martín-Castellanos C, et al. (2005) A large-scale screen in *S. pombe* identifies seven novel genes required for critical meiotic events. *Curr Biol* 15:2056–2062.
25. Dekker J, Rippe K, Dekker M, Kleckner N (2002) Capturing chromosome conformation. *Science* 295:1306–1311.
26. Kim KD, Tanizawa H, Iwasaki O, Noma K (2016) Transcription factors mediate condensin recruitment and global chromosomal organization in fission yeast. *Nat Genet* 48:1242–1252.
27. Fullwood MJ, Ruan Y (2009) ChIP-based methods for the identification of long-range chromatin interactions. *J Cell Biochem* 107:30–39.
28. Wood V, et al. (2002) The genome sequence of *Schizosaccharomyces pombe*. *Nature* 415:871–880, and erratum (2003) 421:94.
29. Tanizawa H, Kim KD, Iwasaki O, Noma KI (2017) Architectural alterations of the fission yeast genome during the cell cycle. *Nat Struct Mol Biol* 24:965–976.
30. Cervantes MD, Farah JA, Smith GR (2000) Meiotic DNA breaks associated with recombination in *S. pombe*. *Mol Cell* 5:883–888.
31. Davis L, Rozalén AE, Moreno S, Smith GR, Martin-Castellanos C (2008) Rec25 and Rec27, novel linear-element components, link cohesin to meiotic DNA breakage and recombination. *Curr Biol* 18:849–854.
32. Estreicher A, Lorenz A, Loidl J (2012) Mug20, a novel protein associated with linear elements in fission yeast meiosis. *Curr Genet* 58:119–127.
33. Zhang L, Kim KP, Kleckner NE, Storlazzi A (2011) Meiotic double-strand breaks occur once per pair of (sister) chromatids and, via Mec1/ATR and Tel1/ATM, once per quartet of chromatids. *Proc Natl Acad Sci USA* 108:20036–20041.
34. Anderson CM, Oke A, Yam P, Zhuge T, Fung JC (2015) Reduced crossover interference and increased ZMM-independent recombination in the absence of Tel1/ATM. *PLoS Genet* 11:e1005478.
35. Cromie GA, Smith GR (2008) Meiotic recombination in *Schizosaccharomyces pombe*: A paradigm for genetic and molecular analysis. *Recombination and Meiosis: Models, Means, and Evolution, Genome Dynamics and Stability*, eds Egel R, Lankenau D-H (Springer, Berlin), pp 195–230.
36. Taylor AF, et al. (2014) Control of RecBCD enzyme activity by DNA binding- and Chi hotspot-dependent conformational changes. *J Mol Biol* 426:3479–3499.
37. Kleckner N, et al. (2004) A mechanical basis for chromosome function. *Proc Natl Acad Sci USA* 101:12592–12597.
38. King JS, Mortimer RK (1990) A polymerization model of chiasma interference and corresponding computer simulation. *Genetics* 126:1127–1138.
39. Fujitani Y, Mori S, Kobayashi I (2002) A reaction-diffusion model for interference in meiotic crossing over. *Genetics* 161:365–372.
40. Hultén MA (2011) On the origin of crossover interference: A chromosome oscillatory movement (COM) model. *Mol Cytogenet* 4:10.
41. Foss E, Lande R, Stahl FW, Steinberg CM (1993) Chiasma interference as a function of genetic distance. *Genetics* 133:681–691.
42. Nambiar M, Smith GR (2016) Repression of harmful meiotic recombination in centromeric regions. *Semin Cell Dev Biol* 54:188–197.
43. de los Santos T, et al. (2003) The Mus81/Mms4 endonuclease acts independently of double-Holliday junction resolution to promote a distinct subset of crossovers during meiosis in budding yeast. *Genetics* 164:81–94.
44. Martini E, Diaz RL, Hunter N, Keeney S (2006) Crossover homeostasis in yeast meiosis. *Cell* 126:285–295.
45. Zhang L, et al. (2014) Topoisomerase II mediates meiotic crossover interference. *Nature* 511:551–556.
46. Egel-Mitani M, Olson LW, Egel R (1982) Meiosis in *Aspergillus nidulans*: Another example for lacking synaptonemal complexes in the absence of crossover interference. *Hereditas* 97:179–187.
47. Sym M, Roeder GS (1994) Crossover interference is abolished in the absence of a synaptonemal complex protein. *Cell* 79:283–292.
48. Berchowitz LE, Copenhaver GP (2010) Genetic interference: Don't stand so close to me. *Curr Genomics* 11:91–102.
49. Ohta K, Wu TC, Lichten M, Shibata T (1999) Competitive inactivation of a double-strand DNA break site involves parallel suppression of meiosis-induced changes in chromatin configuration. *Nucleic Acids Res* 27:2175–2180.
50. Lintern-Moore S, Peters H, Moore GP, Faber M (1974) Follicular development in the infant human ovary. *J Reprod Fertil* 39:53–64.
51. Stahl FW (1993) Genetic recombination: Thinking about it in phage and fungi. *The Chromosome*, eds Heslop-Harrison JS, Flavell RB (Bios Scientific Publishers, Oxford), pp 1–9.
52. Stahl FW, et al. (2004) Does crossover interference count in *Saccharomyces cerevisiae? Genetics* 168:35–48.
53. Cooper TJ, Garcia V, Neale MJ (2016) Meiotic DSB patterning: A multifaceted process. *Cell Cycle* 15:13–21.
54. Smith GR (2009) Genetic analysis of meiotic recombination in *Schizosaccharomyces pombe*. *Meiosis, Methods in Molecular Biology*, ed Keeney S (Humana, Totowa, NJ), pp 65–76.
55. Hyppa RW, Smith GR (2009) Using *Schizosaccharomyces pombe* meiosis to analyze DNA recombination intermediates. *Meiosis, Methods in Molecular Biology*, ed Keeney S (Humana, Totowa, NJ), pp 235–252.
56. Cipak L, Polakova S, Hyppa RW, Smith GR, Gregan J (2014) Synchronized fission yeast meiosis using an ATP analog-sensitive Pat1 protein kinase. *Nat Protoc* 9:223–231.
57. Beach DH, Klar AJS (1984) Rearrangements of the transposable mating-type cassettes of fission yeast. *EMBO J* 3:603–610.
58. Milman N, Higuchi E, Smith GR (2009) Meiotic DNA double-strand break repair requires two nucleases, MRN and Ctp1, to produce a single size class of Rec12 (Spo11)-oligonucleotide complexes. *Mol Cell Biol* 29:5998–6005.
59. Hyppa RW, Cromie GA, Smith GR (2008) Indistinguishable landscapes of meiotic DNA breaks in *rad50*$^{+}$ and *rad50S* strains of fission yeast revealed by a novel *rad50*$^{+}$ recombination intermediate. *PLoS Genet* 4:e1000267.

Supporting Information for

Physical basis for long-distance communication along meiotic chromosomes

Kyle R. Fowler, Randy W. Hyppa, Gareth A. Cromie, and Gerald R. Smith

Supplemental materials and methods

Analysis of DNA proximity by chromosome-conformation capture

DNA isolation. Cells from 500 ml of culture were harvested 3.5 hr after meiotic induction, washed in cold PBS, and incubated in 1% formaldehyde (Sigma) for 5 min at 25°C. Cross-linked cells were opened using a Bead-beater (BioSpec), the chromatin solubilized using a water-bath sonicator (BioRuptor) and centrifuged at 4°C, and the supernatants removed for immunopreciptiation (1). Each chromatin sample was split into two immunoprecipitations, which used magnetic Protein-G beads (Invitrogen) pre-bound with appropriate antibody and incubated with chromatin for 2 hr with rotation at 25°C. Each IP was washed 3x with PBS before being resuspended in 1x Klenow buffer (NEB) supplemented with dNTPs, ATP, and 5 U of Klenow fragment of DNA polymerase I (3' → 5' exo$^-$; NEB) to create blunt ends on the DNA. One of the two IPs was ligated by resuspending the beads in 1 mL of 1x NEB Buffer 2 supplemented with 1 mM ATP and 400 U of T4 ligase (NEB) and incubating with rotation overnight at 4°C; the supernatant was removed and replaced with buffer and 400 U of T4 ligase as before, and incubation continued 2 hr more. Chromatin was eluted twice by incubating the beads in 100 µL of 1% SDS for 15 min at 65°C with frequent vortexing. The second (un-ligated) IP was eluted as above immediately after the binding, washing, and Klenow incubation steps without ligation. For both IPs, formaldehyde cross-links were removed by incubating eluates overnight at 75°C. Protein was subsequently removed using 2 µL of Proteinase K (Invitrogen; 20 mg/mL), and the DNA purified by phenol-chloroform extraction and treatment with RNase A overnight. DNA was cleaned using a PCR purification kit (Qiagen). To the DNA from the second (un-ligated) IP, buffer and 400 U of T4 ligase were added as above and incubated with rotation overnight at 4°C; additional ligase was added as above and incubated 2 hr further before being cleaned using a PCR purification kit (Qiagen). DNA from all samples was amplified using either a Sequenase Version 2.0 DNA Sequencing Kit (for anti-GFP) or a Qiagen REPLI-g Single Cell Kit (for anti-FLAG). DNA was quantified using a Bioanalyzer (Invitrogen).

High-throughput sequencing. Sequencing libraries were each prepared from 1 µg of DNA. DNA was initially fragmented with a Covaris LE220 Focused-ultrasonicator (Covaris, Woburn,

www.pnas.org/cgi/doi/10.1073/pnas.1801920115

MA) using factory settings for an average size of 300 bp. Library DNA was prepared using the KAPA DNA Library Preparation and HiFi PCR Kits (Kapa Biosystems, Wilmington, MA) on a PerkinElmer Sciclone NGSx Workstation (PerkinElmer, Waltham, MA) for Rec25-FLAG and Rec27-FLAG IPs, or the Epicentre Nextera DNA Sample Prep kit (Illumina, Inc., San Diego, CA) manually for Rec27-GFP IPs.

Library DNA size distributions were validated using an Agilent 2200 TapeStation (Agilent Technologies, Santa Clara, CA) and quantified with a Caliper/PerkinElmer LabChip DS spectrophotometer. Additional quality control, blending of pooled indexed libraries, and cluster optimization were performed using Life Technologies' Invitrogen Qubit® 2.0 Fluorometer (Life Technologies-Invitrogen, Carlsbad, CA). Individual indexed libraries were either pooled (4-plex, Rec27-GFP IPs) and clustered onto a single High Output Run flow cell, or pooled (6-plex, Rec25-FLAG and Rec27-FLAG IPs) and clustered onto two lanes of an Illumina Rapid Run v1 flow cell using an Illumina cBot. Sequencing was performed using either an Illumina HiSeq 2000 in High Output Run mode or Illumina HiSeq 2500 in Rapid Run mode using v1 reagents, employing a paired-end, 50-base read length (PE50) sequencing strategy.

Image analysis and base-calling were performed using Illumina's Real Time Analysis software (either v1.12.4 or v1.17.21.3), followed by "demultiplexing" of indexed reads and generation of FASTQ files, using Illumina's CASAVA software (either v1.8.0 or 1.8.2) (http://support.illumina.com/sequencing/sequencing_software/casava.html).

Sequence read mapping. Sequences from each paired-end read were independently mapped to the *S. pombe* genome (downloaded August 2010) using the Burrows-Wheeler Aligner (BWA, v 0.7.9a; (2)) and output as SAM files. We conservatively allowed only a single mismatch per 49 bp sequence (bp 50 was trimmed due to its high inherent error) and kept only sequence pairs where both ends mapped to a single chromosomal position (*i.e.,* a single possible locus of origin). Furthermore, both sequences of a pair had to map to the same chromosome. Alignment files were subsequently imported into R (http://www.r-project.org/) using the Rsamtools package (3) and analyzed using the BioStrings (4) and GenomicRanges (5) packages. Because ~1/3 of each DNA molecule was sequenced (50 bp read per end of each ~300 bp fragment), a significant fraction of all ligation junctions was sequenced. Such molecules would produce a chimeric sequence read, with the 5` portion reflecting one genomic locus and the 3` end another, and would fail to map to the genome based upon our stringent criteria. To capture such events, we iteratively mapped reads failing to map to the genome by trimming the sequence and re-mapping: initially all 49 bp were used, then the 5`-most 25 bp, then the 3`-most 34 bp, and finally the 5`-most 15 bp. Reads that successfully mapped to a single position in the genome were kept, while those that failed were passed to the next iteration;

those that failed to map (or mapped to multiple places) after trimming to 15 bp were set aside. Read-pairs that successfully mapped to the genome after these iterations were pooled and used in subsequent analyses and plots. The results reported here were validated using only reads that mapped on the first iteration (*i.e.,* using all 49 bp).

Filtering intra-molecular interactions. DNA ligation events are relatively rare, with most sequences being of non-ligated DNA. These read-pairs reflect the length of the DNA molecules in the sequencing libraries (~300 bp), while all inter-molecular ligations will give rise to molecules with a larger apparent size. Most ligation events are predicted to arise from intra-molecular interactions (*i.e*., DNA circularization, based upon the close proximity of sonicated DNA ends), and should be removed from further analysis. The map distance between sequence read-pairs derived from circularized molecules reflects the length of sheared meiotic chromatin, the DNA length at the time of ligation. Thus, filtering reads with an apparent length less than the shear length of meiotic chromatin will remove reads of non-ligated and intra-molecular ligation products. To this end, we determined the length distribution of the DNA molecules at the time of ligation by analyzing the map distance between paired reads that map to the same DNA strand (Figure S6A). Such molecules must have arisen from the ligation of DNA ends, of separate molecules, many of which are very distant in the linear genome (Figure S6B). We next binned all paired reads based on their map distance (*e.g.,* reads <200 bp apart, <300 bp, *etc*.) and plotted the fraction of each bin that mapped to the same strand and therefore arose by ligation (Figure S6C). Very close sequence pairs (<300 bp) almost exclusively map to opposite strands, as expected for sequencing primarily intact DNA duplexes (*i.e.,* unligated DNA). Longer reads, up to ~2 kb, are a mixture of same and opposite-stranded reads due to both inter- and intra-molecular ligations, respectively. ~50% of pairs very far apart (>2 kb) are same-stranded due to their arising almost exclusively from inter-molecular ligations, which can give rise to either sequence orientation with equal probability (unlike intra-molecular ligations); the other ~50% also result from inter-molecular ligations but in the other orientation and thus give rise to opposite-strand sequences. Together, these results indicate that sequence pairs <2 kb are biased by intra-molecular interactions. Note that this suggests a DNA size distribution (with most DNA <2 kb), which agrees well with previous results using identically sheared DNA. In all subsequent analyses, paired reads with a map distance <2 kb were excluded.

Hotspot interactions. Positions of published DSB hotspots in *S. pombe* (6) were used to identify sequence pairs where one, both, or neither paired-end read corresponded to hotspot DNA. Sequence-read map positions were compared with hotspot start and end positions, and sequences where at least one end came from a hotspot were pooled. Sequence pairs mapping to different hotspots indicated hotspot interactions; pairs where only one sequence mapped to hotspot DNA, and

the other to cold DNA, may reflect strong competition (*e.g*., sites around *mbs1* or *ade6-3049* where breakage is apparent only in the absence of these hotspots and thus were considered cold DNA).

We first assessed these interactions by looking at an individual hotspot, *ade6-3049* (Figures 1B and 4B). We used the published hotspot start and end positions, ± 2 kb to account for the sheared DNA maximal length, and identified sequence pairs where at least one read mapped inside the hotspot. A cumulative curve was generated from these reads based upon the distance between paired ends (Figure 4D). This was repeated for all hotspots in the genome, and the mean cumulative distribution determined (Figure 4F). This aggregate hotspot analysis was repeated using each sequencing dataset (Figure 4F and Figure S6D).

We next performed a statistical analysis on different subsets of hotspot-associated sequence pairs based upon the distance between reads and whether or not the paired sequence is also from a hotspot. We first identified sequences within ± 2 kb of each hotspot in the genome and grouped these based upon where the other paired sequence mapped (in a hotspot or in a cold-region) and its distance (<100 kb or >100 kb). For each hotspot, the number of sequences in each group (*e.g.,* pairs with one read in the hotspot being analyzed and the other in a hotspot <200 kb away) was normalized by the frequency expected if the paired ends were randomly placed in the appropriate vicinity (*e.g*., the fraction of DNA that occurs in hotspots within a 200 kb interval around the hotspot being analyzed). This procedure accounts for cold-region DNA being much more abundant genome-wide and that 200 kb, a small fraction of each chromosome, should contribute relatively few interactions compared to the rest of the chromosome. The interaction frequencies of each group were then compared using a paired t-test to determine statistical significance (Figure 4G).

Construction of *mbs1-20* deletion

Oligonucleotides 1018 and 1019 were used with *S. pombe* genomic DNA as template to make a PCR product ~500 bp long at the left end of the *mbs1-20* deletion; a similar PCR product at the right end was generated using oligonucleotides 1021 and 1022 with *S. pombe* genomic DNA as template. Oligonucleotides 1019 and 1021 are complementary. The two PCR products, plus oligonucleotides 1018 and 1022, were used to generate a PCR product ~1 kb long, which was used to transform strain GP4126 (*mbs1-1::ura4*$^{+}$) to 5-fluoro-orotic acid (FOA)-resistance. A transformant, GP4253, was purified and confirmed by nucleotide sequence analysis to contain the 6.6 kb deletion designated *mbs1-20*, which was transferred from GP4253 to other strains by meiotic crosses.

Construction of *rec25::FLAG* and *rec27::FLAG* alleles

DNA oligos with 80 bp of homology to the left and right of the ORF of either *rec25* (OL3169 and OL3170) or *rec27* (OL3171 and OL3172) were used to amplify a *2FLAG-kanMX6* cassette sequence from *S. pombe* strain GP7932 (*cnp20-2FLAG::kanM6*). The resulting PCR products were purified and used to transform *S. pombe* strain GP5623 to G418-resistance on YEA (7). The alleles *rec25-221::2FLAG-kanMX6* in strain GP8112 and *rec27-222::2FLAG-kanMX6* in strain GP8113 were verified by PCR and sequencing; they were transferred to other strains by meiotic crosses.

References

1. Fowler KR, Gutiérrez-Velasco S, Martín-Castellanos C, & Smith GR (2013) Protein determinants of meiotic DNA break hotspots. *Mol. Cell* 49:983-996.
2. Li H & Durbin R (2009) Fast and accurate short read alignment with Burrows-Wheeler transform. *Bioinformatics* 25(14):1754-1760.
3. Morgan MT, Pagès H, Obenchain V, & Hayden N (2016) Rsamtools: Binary alignment (BAM), FASTA, variant call (BCF), and tabix file import. R package version 1.24.0.
4. Pagès H, Aboyoun P, Gentleman R, & DebRoy S (2016) Biostrings: String objects representing biological sequences, and matching algorithms. R package version 2.40.2.
5. Lawrence M*, et al.* (2013) Software for computing and annotating genomic ranges. *PLoS Comput Biol* 9(8):e1003118.
6. Fowler KR, Sasaki M, Milman N, Keeney S, & Smith GR (2014) Evolutionarily diverse determinants of meiotic DNA break and recombination landscapes across the genome. *Genome Research* 24:1650-1664.
7. Bähler J*, et al.* (1998) Heterologous modules for efficient and versatile PCR-based gene targeting in *Schizosaccharomyces pombe*. *Yeast* 14:943-951.
8. Smith GR (2009) Genetic analysis of meiotic recombination in *Schizosaccharomyces pombe*. *Meiosis,* Methods in Molecular Biology, ed Keeney S (Humana Press, Totowa, NJ), pp 65-76.
9. Zahn-Zabal M, Lehmann E, & Kohli J (1995) Hot spots of recombination in fission yeast: inactivation of the *M26* hot spot by deletion of the *ade6* promoter and the novel hotspot *ura4-aim*. *Genetics* 140:469-478.
10. Baur M*, et al.* (2005) The meiotic recombination hot spot *ura4A* in *Schizosaccharomyces pombe*. *Genetics* 169(2):551-561.
11. Steiner WW & Smith GR (2005) Optimizing the nucleotide sequence of a meiotic recombination hotspot in *Schizosaccharomyces pombe*. *Genetics* 169(4):1973-1983.
12. Tanaka K, Chang HL, Kagami A, & Watanabe Y (2009) CENP-C functions as a scaffold for effectors with essential kinetochore functions in mitosis and meiosis. *Developmental cell* 17(3):334-343.
13. Cromie GA, Rubio CA, Hyppa RW, & Smith GR (2005) A natural meiotic DNA break site in *Schizosaccharomyces pombe* is a hotspot of gene conversion, highly associated with crossing over. *Genetics* 169:595-605.
14. Iino Y & Yamamoto M (1985) Mutants of *Schizosaccharomyces pombe* which sporulate in the haploid state. *Molecular and General Genetics* 198:416-421.
15. Guerra-Moreno A, Alves-Rodrigues I, Hidalgo E, & Ayte J (2012) Chemical genetic induction of meiosis in *Schizosaccharomyces pombe*. *Cell Cycle* 11(8):1621-1625.
16. Farah JA, Hartsuiker E, Mizuno K-I, Ohta K, & Smith GR (2002) A 160-bp palindrome is a Rad50•Rad32-dependent mitotic recombination hotspot in *Schizosacchromyces. pombe*. *Genetics* 161:461-468.

17. Farah JA, Cromie G, Davis L, Steiner WW, & Smith GR (2005) Activation of an alternative, Rec12 (Spo11)-independent pathway of fission yeast meiotic recombination in the absence of a DNA flap endonuclease. *Genetics* 171(4):1499-1511.
18. Davis L & Smith GR (2003) Non-random homolog segregation at meiosis I in *Schizosaccharomyces pombe* mutants lacking recombination. *Genetics* 163:857-874.
19. Davis L, Rozalén AE, Moreno S, Smith GR, & Martin-Castellanos C (2008) Rec25 and Rec27, novel components of meiotic linear elements, link cohesin to DNA breakage and recombination in fission yeast. *Current Biology* 18:849-854.
20. Grimm C, Bahler J, & Kohli J (1994) *M26* recombinational hotspot and physical conversion tract analysis in the *ade6* gene of *Schizosaccharomyces pombe*. *Genetics* 135:41-51.
21. Hyppa RW & Smith GR (2009) Using *Schizosaccharomyces pombe* meiosis to analyze DNA recombination intermediates. *Meiosis,* Methods in Molecular Biology, ed Keeney S (Humana Press, Totowa, NJ), pp 235-252.
22. Hyppa RW, Cromie GA, & Smith GR (2008) Indistinguishable landscapes of meiotic DNA breaks in *rad50*$^{+}$ and *rad50S* strains of fission yeast revealed by a novel *rad50*$^{+}$ recombination intermediate. *PLoS Genet* 4(11):e1000267.
23. Cromie GA*, et al.* (2007) A discrete class of intergenic DNA dictates meiotic DNA break hotspots in fission yeast. *PLoS Genetics* 3:e141.

Table S1. Positive DSB interference in *tel1*$^{+}$ strains but negative DSB interference in *tel1Δ* strains: interference weakens with distance in the 15 – 250 kb range.

		***tel1*$^{+}$**					***tel1Δ***				
Distance between hotspots (kb)[1]	**Supple-mental Figure**	**DSB1**	**DSB2**	**2X cut obs**	**2X cut exp**	**I**	**DSB1**	**DSB2**	**2X cut obs**	**2X cut exp**	**I**
15-20	Figure 3 B&C[2]	5.8 +/-0.26	9.0 +/-0.55	0.2 +/-0.1	0.52 +/-0.05	0.64 +/-0.14	6.0 +/-0.38	11.8 +/-0.58	2.6 +/-0.39	0.71 +/-0.08	-2.6 +/-0.32
	3 B&C	5.8	8.0	0.1	0.46	0.81	9.4	10.0	2.1	0.90	-1.3
	3 D&E	6.1 +/-0.48	8.8 +/-0.86	0.1 +/-0.009	0.53 +/-0.09	0.84 +/-0.04	5.9 +/-0.40	10.5 +/-0.18	2.4 +/-0.31	0.62 +/-0.05	-3.0 +/-0.75
20-25 (*ura2-leu2*)	5 B (a – b)[3]	4.92 +/-0.56	5.05 +/-0.68	0.12 +/-0.002	0.25 +/-0.06	0.52 +/-0.05	5.0 +/-0.39	5.26 +/-0.65	0.58 +/-0.058	0.26 +/-0.04	-1.32 +/-0.43
45	3 B&C	ND[4]					7.3	7.7	2.5	0.56	-3.5
	3 D&E						3.8	6.6	1.1	0.25	-3.4
95	5 B (a – c)	4.92 +/-0.56	11.42 +/-0.93	0.83 +/-0.006	0.57 +/-0.1	-0.61 +/-0.45	5.0 +/-0.39	12.75 +/-0.55	1.92 +/-0.34	0.64 +/-0.007	-2.16 +/-0.87
100 (*mbs1-2*)	5 A (*mbs1-2*)	10.43 +/-1.03	3.3 +/-0.18	0.18 +/-0.02	0.35 +/-0.05	0.46 +/-0.06	13.16 +/-0.26	4.38 +/-0.22	0.49 +/-0.009	0.59 +/-0.04	0.16 +/-0.07
125	5 D (d – e)	3.6	9.3	0.31	0.33	0.06	3.2	11.9	0.8	0.38	-1.1
		3.3	8.8	0.20	0.29	0.31	3.1	11.7	0.55	0.36	-0.5
250	5 D (f – g)	7.1	8.7	0.40	0.62	0.35	8.0	11.7	0.89	0.94	0.05
		8.1	10.0	0.54	0.81	0.33	8.5	15.9	0.80	1.3	0.38

[1] Distances were determined from the genome-wide analysis of DSB hotspots (1, 6) and the *S. pombe* genome sequence (https://www.pombase.org/).

[2] Main text Figure 3B and 3C.

[3] DSB hotspot pairs assayed for double-cut fragments are in parentheses.

[4] The 45 kb interval could not be measured because the left DSB hotspot is created by *tel1Δ*.

Data are the percent of total DNA cut at each hotspot (DSB1 and DSB2) and at both hotspots (2X cut obs). 2X cut exp is the percent cut at both hotspots expected from independent breakage (DSB1 times DSB2). Interference I = 1 – (2x cut obs/2x cut exp). Data are from the experiments shown in

the indicated figures. Values are mean ± SEM for three or more determinations, or individual values for one or two determinations.

Table S2. Crossover interference

A. Intra-chromosomal interference – strongly negative in *tel1Δ* mutants and weakly positive in wild type

tel1	R_1	R_2	R_D	Expected R_D	CoC	I[a]
+	3.40	13.0	0.32	0.44	0.72	0.28
+	3.12	12.2	0.34	0.38	0.89	0.11
+	4.68	20.00	0.62	0.94	0.66	0.34
+	3.84	23.3	0.74	0.89	0.83	0.17
+	3.78	18.9	0.44	0.71	0.62	0.38
mean	3.76	17.5	0.49	0.67	0.74	**+0.26**
± SEM	± 0.26	± 2.1	± 0.08	± 0.11	± 0.051	**± 0.051**
Δ	3.26	8.84	0.56	0.29	1.93	-0.93
Δ	3.78	8.58	0.66	0.32	2.06	-1.06
Δ	3.16	10.0	0.56	0.32	1.75	-0.75
Δ	3.16	9.70	0.56	0.31	1.81	-0.81
Δ	2.66	6.54	0.30	0.17	1.76	-0.76
Δ	2.58	6.90	0.34	0.18	1.89	-0.89
Δ	2.78	5.86	0.34	0.16	2.13	-1.13
Δ	2.78	7.56	0.40	0.21	1.90	-0.90
mean	3.02	8.00	0.47	0.245	1.90	**-0.90**
± SEM	± 0.14	± 0.54	± 0.048	± 0.025	± 0.048	**± 0.048**

[a] In additional crosses conducted with different strains on different days (Table S2B and S2C and other crosses), I = 0.29 ± 0.043 (n = 12) for *tel1*$^+$ and -0.80 ± 0.14 (n = 8) for *tel1Δ.*

For part A. Crosses were conducted between strains GP77 and GP7144 (*tel1*$^+$) and between strains GP9019 and GP9022 (*tel1Δ*). Each pair had *ura2-10* + *lys7-2* and + *leu2-120* +, linked loci on chromosome I. Recombinant frequencies (twice the observed % of selected prototrophs among total viable spores) were determined by differential plating on appropriately supplemented NBA minimal medium. In the tested subset of both wt and *tel1Δ* crosses, ~10% of the double recombinants were complementing diploids (iodine-staining positive) (8). Thus, R_D and CoC may be ~5% less than shown here, and I would be about +0.27 for wt and about -0.92 for *tel1Δ*. This minor correction would not change our conclusions. More than 22 and usually more than 100 colonies were counted for each determination. The coefficient of coincidence (CoC) is $R_D/(R_1 \times R_2)$, where R_1 is twice the frequency of Ura$^+$ Leu$^+$ recombinants, R_2 is twice the frequency of Leu$^+$ Lys$^+$ recombinants, and R_D is twice the frequency of Ura$^+$ Leu$^+$ Lys$^+$ recombinants. Expected R_D is $(R_1 \times R_2)$. Interference (I) is 1 - CoC. These data are summarized in Table 1.

B. No significant inter-chromosomal crossover interference – *tel1*$^+$

Interval 3 (Chr 2)	CO interval 1 (%)	CO interval 2 (%)	CO interval 3 (%)	Double CO 1 and 2 (%)	Double CO 1 and 3 (%)	Double CO 2 and 3 (%)
ade7 – arg6	2.70 ± 0.060	11.52 ± 0.82	11.24 ± 0.90	0.232 ± 0.050	0.290 ± 0.035	1.25 ± 0.060
Interference				**0.24** ± 0.07	**0.04** ± 0.17	**0.03** ± 0.16
arg4 – arg5	2.62 ± 0.114	9.52 ± 0.48	4.64 ± 0.066	0.172 ± 0.012	0.127 ± 0.017	0.420 ± 0.052
Interference				**0.31** ± 0.04	**- 0.04** ± 0.13	**0.05** ± 0.11

C. No significant inter-chromosomal crossover interference – *tel1Δ*

Interval 3 (Chr 2)	CO interval 1 (%)	CO interval 2 (%)	CO interval 3 (%)	Double CO 1 and 2 (%)	Double CO 1 and 3 (%)	Double CO 2 and 3 (%)
ade7 – arg6	2.58 ± 0.16	7.36 ± 0.48	8.42 ± 0.096	0.344 ± 0.060	0.264 ± 0.017	0.668 ± 0.064
Interference				**-0.81** ± 0.25	**-0.22** ± 0.12	**-0.08** ± 0.11
arg4 – arg5	2.74 ± 0.26	6.50 ± 0.30	4.36 ± 0.13	0.316 ± 0.024	0.130 ± 0.014	0.278 ± 0.014
Interference				**-0.77** ± 0.17	**-0.09** ± 0.040	**0.02** ± 0.12

For parts B and C. Crosses were conducted between *tel1*$^+$ strains GP9443 and GP9445 (*ade7 – arg6*, linked loci on chromosome 2), between *tel1*$^+$ strains GP9453 and GP9449 (*arg4 – arg5,* linked loci on chromosome 2), between *tel1Δ* strains GP9442 and GP9444 (*ade7 – arg6*), and between *tel1Δ* strains GP9452 and GP9446 (*arg4 – arg5*); these strain pairs also contained the *ura2, leu2,* and *lys7* alleles linked on chromosome 1 as in part A. Recombinant frequencies were determined as in part A, except that differential plating was on appropriately supplemented PMG minimal medium. Recombinant frequencies for interval 1 and 3 (or 2 and 3) double recombinants are four times the

observed % of selected prototrophs among total viable spores. Except in a few cases, between 100 and 300 colonies were counted for each determination. Data are the mean ± SEM from four crosses with independent cultures.

Table S3. DSB frequencies at the *ura4A* and *ade6-3049* hotspots, alone and in combination.

DSB hotspot	+ + / - -	+ - / - +	+ - / + -	+ - / - -	- + / - +	- + / - -	+ + / + +
ura4A$^+$	1.8, 1.8, 1.45, 1.55 **1.65** ± 0.09	3.2, 3.05, 3.13, 2.87 **3.06** ± 0.07	6.3, 7.2, 6.25 **6.6** ± 0.3	4.0, 3.12, 3.65 **3.6** ± 0.3	0.2, 0.3, 0.1 **0.2** ± 0.06	0.2, 0.3, 0.1 **0.2** ± 0.06	1.4, 1.35, 2.1, 2.15 **1.75** ± 0.2
ade6-3049	8.9, 7.9, 9.0, 9.5 **8.83** ± 0.34	7.7, 7.8, 9.0, 9.1 **8.40** ± 0.38	0.1, 0.3, 0.1 **0.2** ± 0.07	0.3, 0.25, 0.1 **0.22** ± 0.06	12.2, 13.8, 14.9 **13.6** ± 0.8	5.55, 7.3, 5.6 **6.2** ± 1.0	13.2, 11.4, 18.2, 17.5 **15.1** ± 1.9
tel1::kanMX6	5.36, 4.38, 4.55, 4.80, 3.83, 2.87 **4.30** ± 0.35	5.0, 4.88, 5.80, 5.30, 3.70, 3.32 **4.67** ± 0.39		6.10, 4.05, 3.05 **4.40** ± 0.90		0.10, 0.40, 0.10 **0.20** ± 0.10	
ade6-3049	3.90, 3.01, 6.70, 4.50, 3.78, 4.22 **4.35** ± 0.51	7.51, 5.92, 10.60, 6.45, 5.65, 6.70 **7.14** ±0.74		0.15, 0.30, 0.1 **0.18** ± 0.06		7.28, 7.80, 5.30 **6.79** ± 0.76	

Strains induced for meiosis had the configuration of the *ura4A*, *tel1::kanMX6*, or *ade6-3049* hotspots shown in the top line as in Figure 2, *ura4A*$^+$ or *tel1::kanMX6* on the left and *ade6-3049* on the right. + indicates an active hotspot; - indicates no hotspot (lacking the *ura4A*$^+$ insertion or the *tel1::kanMX6* substitution, or containing the non-hotspot allele *ade6-3057*) (9, 10); (11). Data are the percent of total DNA broken at the *ura4A*$^+$*, tel1::kanMX6,* or *ade6-3049* hotspot determined in Southern blot hybridization analyses as in Figures 2 (top two sets of data) and S2 (bottom two sets of data). In bold is the mean, followed by the SEM.

Table S4. Genotypes of *S. pombe* strains.

Strain	Genotype[1]	Used in
GP7256	*h⁻/h⁻ ade6-3049/ade6-3049 pat1-114/pat1-114 rec27-205::GFP-kanMX6/rec27-205::GFP-kanMX6 rec12-169::kanMX6/rec12-169::kanMX6 his4-239/+ +/lys4-95*	Figures 1, 4, S8-S10
GP9246	*h+/h+ ade6-3049/ade6-3049 pat1-114/pat1-114 rec12-201::6His2FLAG/rec12-201::6His2FLAG rad50S/rad50S his4-239/lys4-95*	Figure 2
GP9305	*h+/h+ ade6-3049/ade6-3057 pat1-114/pat1-114 rec12-201::6His2FLAG/rec12-201::6His2FLAG rad50S/rad50S mbs1-20/+ his4-239/lys4-95*	Figures 2 and S2
GP9337	*h+/h+ ade6-3057/ade6-3049 +/ura4A pat1-114/pat1-114 rec12-201::6His2FLAG/+ rad50S/rad50S ura4-D18/ura4-D18 his4-239/lys4-95*	Figure 2
GP9338	*h+/h+ ade6-3057/ade6-3057 ura4A/ura4A pat1-114/pat1-114 rad50S/rad50S ura4-D18/ura4-D18 his4-239/lys4-95*	Figure 2
GP9339	*h+/h+ ade6-3049/ade6-3057 +/ura4A pat1-114/pat1-114 rec12-201::6His2FLAG/+ rad50S/rad50S ura4-D18/ura4-D18 his4-239/lys4-95*	Figure 2
GP9340	*h+/h+ ade6-3057/ade6-3057 +/ura4A pat1-114/pat1-114 rec12-201::6His2FLAG/+ rad50S/rad50S ura4-D18/ura4-D18 his4-239/lys4-95*	Figure 2
GP8828	*h^{90} rec10-203::GFP-kanMX6*	Figures 5 and S14
GP8824	*h^{90} rec25-204::GFP-kanMX6*	Figures 5 and S14
GP8826	*h^{90} rec27-205::GFP-kanMX6*	Figures 5 and S14
GP9036	*h^{90} rec10-203::GFP-kanMX6 tel1::kanMX6*	Figures 5 and S14
GP9033	*h^{90} rec25-204::GFP-kanMX6 tel1::kanMX6*	Figures 5 and S14
GP9034	*h^{90} rec27-205::GFP-kanMX6 tel1::kanMX6*	Figures 5 and S14
GP8907	*h⁺/h⁺ ade6-3049/ade6-3049 ura4⁺-aim/ura4⁺-aim pat1-114/pat1-114 tel1::kanMX6/tel1::kanMX6 rad50S/rad50S his4-239/+ +/lys4-95*	Figures 2, S2, S3 and S5
GP8908	*h⁻/h⁻ ade6-3049/ade6-3049 ura4⁺-aim/ura4⁺-aim pat1-114/pat1-114 rad50S/rad50S his4-239/+ +/lys4-95*	Figures S2, S3 and S5
GP8909	*h⁻/h⁻ ade6-3049/ade6-3049 ura4⁺-aim/ura4⁺-aim pat1-as1*(L95G)*/pat1-as1*(L95G) *rad50S/rad50S his4-239/+ +/lys4-95*	Figures 3, S2, S3, and S4
GP8910	*h⁻/h⁻ ade6-3049/ade6-3049 ura4⁺-aim/ura4⁺-aim pat1-as1*(L95G)*/pat1-as1*(L95G) *tel1::kanMX6/tel1::kanMX6 rad50S/rad50S his4-239/+ +/lys4-95*	Figures 3, S2, S3, and S4
GP8663	*h⁻/h⁻ ade6-3049/ade6-3049 pat1-114/pat1-114 rec27-205::GFP-kanMX6/rec27-205::GFP-kanMX6 rec8-176::kanMX/rec8-176::kanMX his4-239/+ +/lys4-95*	Figure 4 and S13
GP8237	*h⁻/h⁻ ade6-3049/ade6-3049 ura4-D18/+ pat1-114/pat1-114 rec12-171::ura4⁺/rec12-171::ura4⁺ rec25-221::2FLAG/rec25-221::2FLAG his4-239/+ +/lys4-95 +/leu1-32*	Figure S6
GP8240	*h⁻/h⁻ ade6-3049/ade6-3049 pat1-114/pat1-114 rec12-171::ura4⁺/rec12-171::ura4⁺ rec27-222::2FLAG/rec27-222::2FLAG his4-239/+ +/lys4-95 +/leu1-32*	Figure S6
GP7062	*h⁺/h⁺ ade6-3057/ade6-3057 pat1-114/pat1-114 rec12-201::6His-2FLAG/rec12-201::6His-2FLAG rad50S/rad50S lys4-95/+ +/his4-239*	Figures 1B, 1C, 1D, and S1
GP6852	*h⁺/h⁺ ade6-3049/ade6-3049 pat1-114/pat1-114 rec12-201::6His-2FLAG/rec12-201::6His-2FLAG rad50S/rad50S mbs1-20/mbs1-20 his4-239/+ +/lys4-95*	Figures 1B,1C, 1D, and S1
GP77	*h⁻ leu2-120*	Tables 1 and S2
GP7144	*h⁺ ura2-10 lys7-2*	Tables 1 and S2
GP9019	*h⁺ ura2-10 lys7-2 tel1::kanMX6*	Tables 1 and S2
GP9022	*h⁻ leu2-120 tel1::kanMX6*	Tables 1 and S2
GP9443	*h- ura2-10 lys7-2 arg6-328*	Table S2

GP9445	*h+ leu2-120 ade7-50*	Table S2
GP9453	*h+ ura2-10 lys7-2 arg5-189*	Table S2
GP9449	*h- leu2-120 arg4-55*	Table S2
GP9442	*h- ura2-10 lys7-2 arg6-328 tel1::kanMX6*	Table S2
GP9444	*h+ leu2-120 ade7-50 tel1::kanMX6*	Table S2
GP9452	*h+ ura2-10 lys7-2 arg5-189 tel1::kanMX6*	Table S2
GP9446	*h- leu2-120 arg4-55 tel1::kanMX6*	Table S2
GP4126	*h^+ ade6-3049 ura4-D18 mbs1-1::ura4$^+$ pat1-114 rad50S end1-458*	*mbs1-20* construction
GP9343	*h^+/h^+ ade6-3057/ade6-3049 pat1-114/pat1-114 rad50S/rad50S rec12-201::6His-2FLAG/rec12-201::6His-2FLAG +/tel1::kanMX6 his4-239/lys4-95 +/mbs1-20*	Figure S2
GP9344	*h^+/h^+ ade6-3057/ade6-3057 pat1-114/pat1-114 rad50S/rad50S rec12-201::6His-2FLAG/rec12-201::6His-2FLAG +/tel1::kanMX6 his4-239/lys4-95 mbs1$^+$/mbs1$^+$*	Figure S2
GP9345	*h^+/h^+ ade6-3049/ade6-3057 pat1-114/pat1-114 rad50S/rad50S rec12-201::6His-2FLAG/rec12-201::6His-2FLAG +/tel1::kanMX6 his4-239/lys4-95 mbs1-20/+*	Figure S2
GP7932	*h^- leu1 ade6 cnp20::2FLAG-kanMX6*	*rec25-221 and rec27-222* constructions
GP5623	*h^+ ade6-3049 ura4-D18 rec12-171::ura4$^+$*	*rec25-221 and rec27-222* constructions

[1] Strains were constructed by standard matings (8) or as described in Methods. Genealogies are available upon request. Sources of alleles, other than commonly used auxotrophies and *mat*, are the following: *ade6-3049* (11); *cnp20::2FLAG-kanMX6* (12); *mbs1-1::ura4*$^+$ (13); *mbs1-20* (Methods); *pat1-114* (14); *pat1-as1*(L95G) (15); *rad50S* (16); *rec8-176::kanMX* (17); *rec10-203::GFP-kanMX6* (1); *rec12-169::kanMX6* (18); *rec12-171::ura4*$^+$ (18); *rec25-204::GFP-kanMX6* (19); *rec25-221::2FLAG-kanMX6* (Methods); *rec27-205::GFP-kanMX6* (19); *rec27-222::2FLAG-kanMX6* (Methods); *tel1::kanMX6* (Y. Yamada, O. Limbo, P. Russell); *ura4A* (also called *ura4*$^+$*-aim* (20).

Table S5. Oligonucleotides.

Oligo number	Sequence (5' → 3')	Use
1401	GGATGGCTGCCCCTTCGTCTCG	Probe for Figure 2
1402	GGCTAACACTTATCAACGCG	Probe for Figure 2
2576	TTCCATCTTCAGCTCCCACT	Probe for Figures 3B and S2
2577	CGAGGACTTGCAATTGTCTG	Probe for Figures 3B and S2
2779	TGGTTTCTCTCAATCCCTTA	Probe for Figure S3
2780	TTACACACTTTACCCCGTTC	Probe for Figure S3
1018	GGCATAGTCCAATTCGCGCG	*mbs1-20* deletion
1019	GCTCACTTGCCCTAAGCTCACGTTCCCATAGGCCAGCAATTCCC	*mbs1-20* deletion
1021	GGGAATTGCTGGCCTATGGGAACGTGAGCTTAGGGCAAGTGAGC	*mbs1-20* deletion
1022	GCAATGGGCTTCGTGGGAGC	*mbs1-20* deletion
3126	AAGTATTAGAAGAAGATGGATCGCAGCAAGGGTCTCAGCTTATACA AGGGCTGCTAACGTGTTTTCAATCTACTGGTAATCGGATCCCCGGG TTAATTAA	Construction of *rec25-221::2FLAG-kanMX6*
3127	GACAATTAATAACATTTAGATGAAAAAGTAGTAGAGTTGGAATAAAT TTAGCTTTGAGTTTCAATCGTAATTTAGCTTATGAATTCGAGCTCGTT TAAAC	Construction of *rec25-221::2FLAG-kanMX6*
3128	GCAATCAGTTGTTACAGTATGCCGAGAAACTGCGAATTGTTGTTAAA ACCCCAATGAACCAACCAACAAATACAGAAGTACGGATCCCCGGGT TAATTA	Construction of *rec27-222::2FLAG-kanMX6*
3129	TAAATTGTATGCTCATAACATATTTTTAATTCGTTTTATGATTTTATGG CACTAGTTTATATAATGTGTTTAAAATGACTGAATTCGAGCTCGTTTA AAC	Construction of *rec27-222::2FLAG-kanMX6*

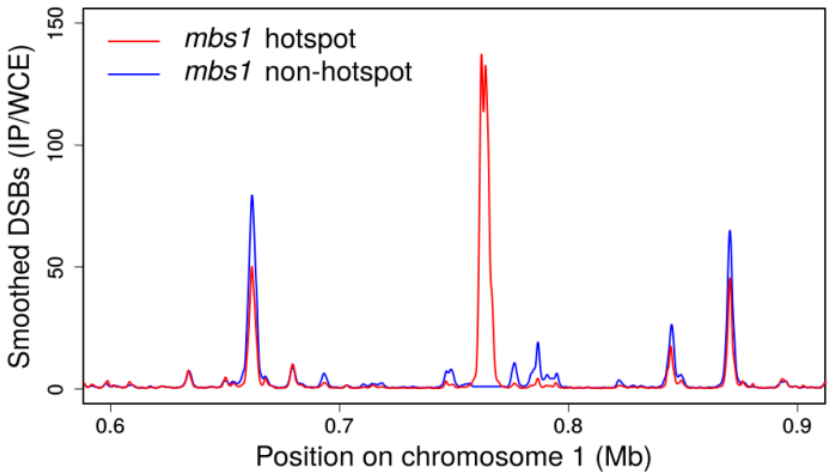

Figure S1. DSB competition and clustering at the natural DSB hotspot *mbs1* occur in *tel1*$^{+}$ cells. DSB frequency is reduced at hotspots within ~100 kb of the *mbs1* natural hotspot (13). See Figures 1 and 4 for further explanation. DSB frequency on part of chromosome 1 in *mbs1*$^{+}$ (wild-type) cells with a DSB hotspot (red line) and in the 6.6 kb *mbs1-20* deletion mutant without a hotspot (blue line). Data were median normalized separately (see Figure 1C). Note that low-level sites for DSBs in wild-type become stronger DSB hotspots in the absence of *mbs1*, a reflection of DSB competition.

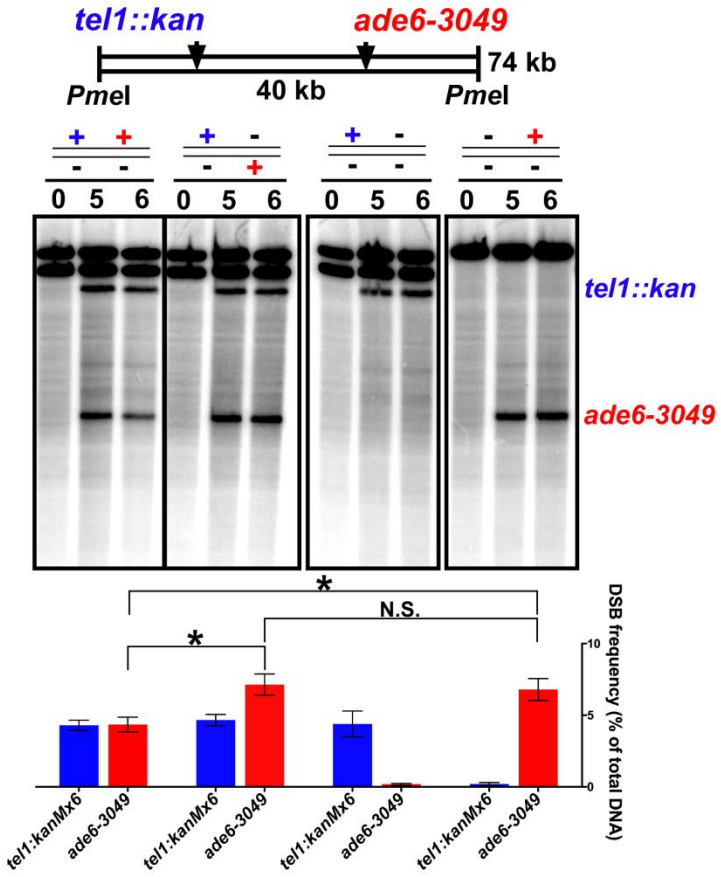

Figure S2. DSB competition acts along a homolog (in *cis*) but not between homologs (in *trans*). The *tel1::kan* (blue) and *ade6-3049* (red) DSB hotspots (+) were located either on the same parental homolog (in *cis*; left-most set of lanes) or on different parental homologs (in *trans*, second set of lanes); - indicates lack of a hotspot. In comparison experiments, one hotspot or the other was present in heterozygous condition (two right-most sets of lanes). Strains GP9343 (*tel1*::*kan ade6-3049/tel1*$^+$ *ade6*$^+$), GP9345 (*tel1*::*kan ade6*$^+$*/tel1*$^+$ *ade6-3049*), GP9344 (*tel1*::*kan ade6*$^+$*/tel1*$^+$ *ade6*$^+$) and GP9305 (*tel1*$^+$ *ade6-3049/tel1*$^+$ *ade6*$^+$) were induced for meiosis by raising the temperature to 34°C. DSBs at each hotspot were assayed at the indicated times after induction. Data (mean ± SEM; n = 3 to 6) are the percent of total DNA broken at the indicated hotspot (assayed with a probe at the right end of the *Pme*I fragment). Comparison of the fourth set of lanes (no *tel1::kan* hotspot) shows that the *ade6-3049* hotspot is significantly reduced when *tel1::kan* is in *cis* (first set of lanes; $p < 0.030$ by unpaired t-test; *) but not significantly reduced when *tel1::kan* is in *trans* (second set of lanes; $p = 0.78$ by unpaired t-test; N.S.). Direct comparison of the first two sets of lanes shows that *tel1::kan* reduces the *ade6-3049* hotspot significantly more in *cis* than in *trans* ($p < 0.011$ by unpaired t-test). See Table S3 for individual data.

\

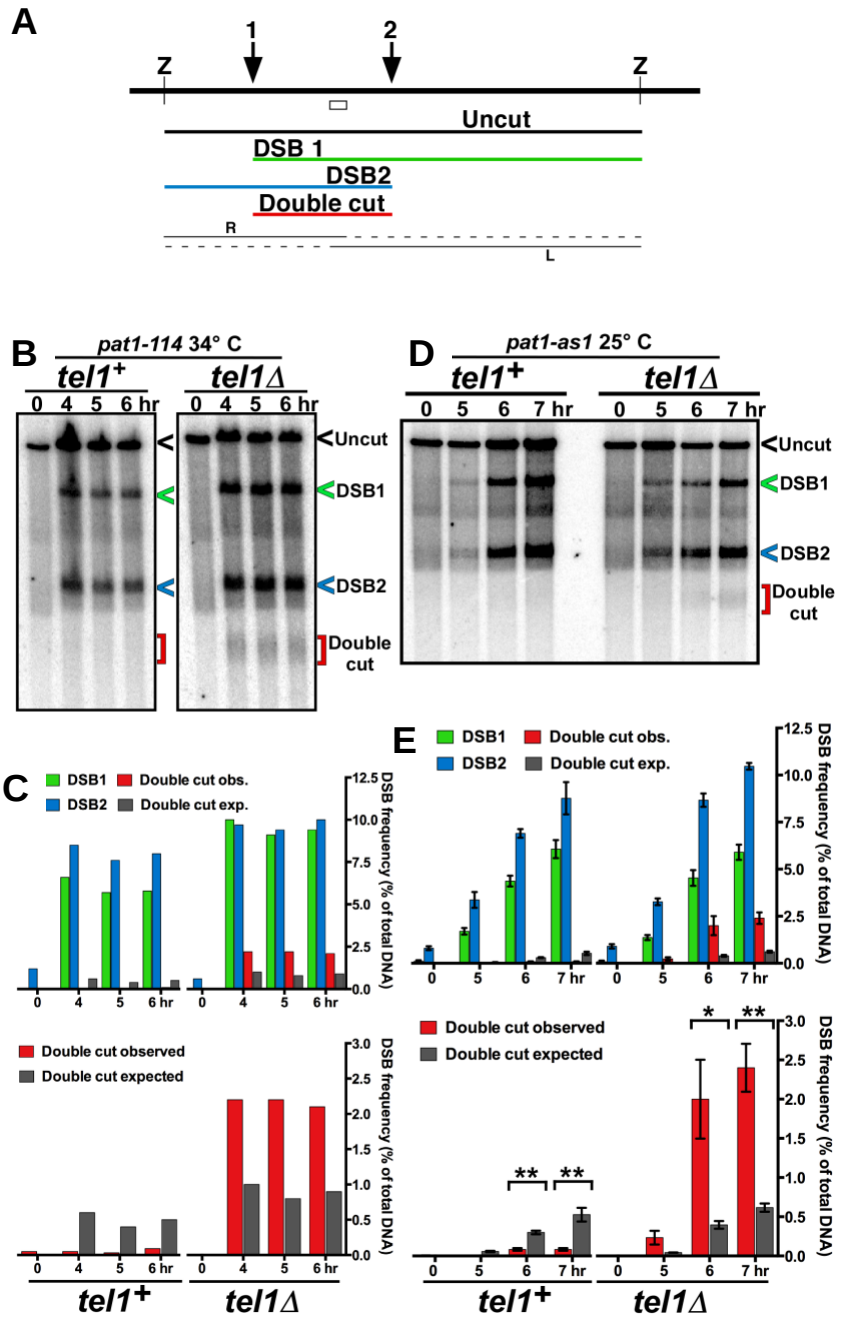

Figure S3. Interference of DSB formation at nearby hotspots depends on Tel1 DNA damage-response protein kinase: Analysis of two hotspots 15 kb apart near the left end of chromosome 2. (**A**) Scheme for determining DSB frequency at one, the other, and both hotspots (1 and 2) by Southern blot hybridization of DNA cut by a restriction enzyme Z; open box, probe position. The *rad50S* mutation, present in all strains, blocks DSB repair and allows their accumulation and quantification (21); DSBs accumulate in *rad50S* mutants with a distribution indistinguishable from that

of wild type (22). DNA fragments cut by Z at one end and by Rec12 at the other end (fragments DSB1 and DSB2) or at both ends by Rec12 (Double-cut fragment) migrate as distinct bands at the positions indicated (green and blue arrowheads for single-cut and red bracket for double-cut). DNA fragments cut at Z and mechanically broken during preparation in the region marked with a dotted line (bottom of scheme) migrate as a smear ending at the position corresponding to the DNA length from the probe to Z on the left or on the right (bands R and L, respectively). This feature accounts for the "rain" ending at distinct positions in the gel. Z was chosen so that the doubly-cut fragment migrates below the rain, enabling its quantification. (**B**) DSB interference between two hotspots on the left end of chromosome 2. Strains GP8908 (*pat1-114 tel1*$^{+}$) and GP8907 (*pat1-114 tel1Δ*) were induced by raising the temperature to 34°C. DNA was extracted at the indicated times, digested with *Avr*II (which cuts at bp 939346 and 993665), and analyzed by Southern blot hybridization using a 0.48 kb radioactive probe near the middle of the 54.3 kb fragment (uncut). (**C**) Quantification of the bands shows that the observed doubly-cut fragment (red bars) is less frequent than expected from independent breakage at the two hotspots (black bars) in wild type but more frequent than expected in *tel1Δ*. *, $p < 0.05$ by unpaired t-test; **, $p < 0.01$ by unpaired t-test. (**D**) Analysis as in panel B but with strains GP8909 (*pat1-as1 tel1*$^{+}$) and GP8910 (*pat1-as1 tel1Δ*) induced at 25°C with the adenine analog 3-MB-PP1 (15). (**E**) Analysis as in panel C of expected and observed double-cut fragments shown in panel D.

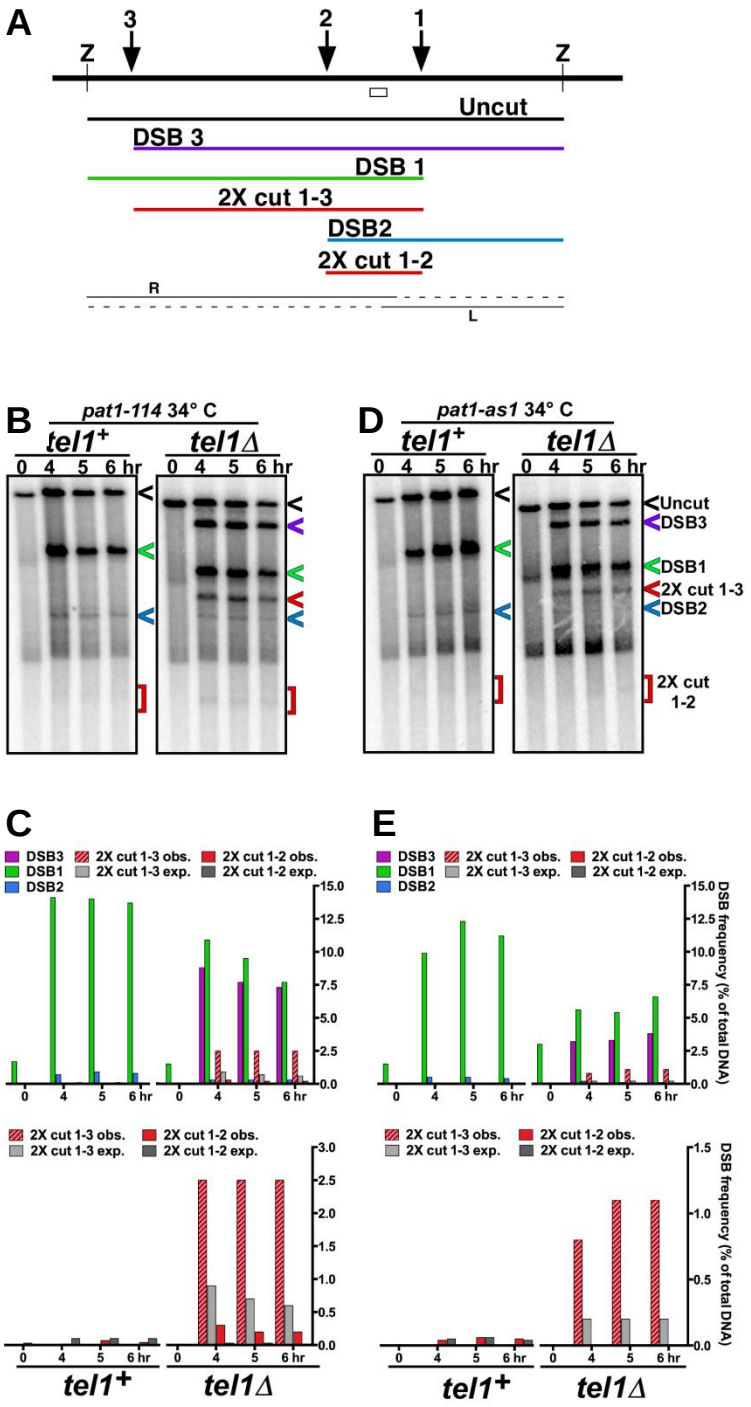

Figure S4. Interference of DSB formation at nearby hotspots depends on Tel1 DNA damage-response protein kinase: Analysis of two hotspots (in *tel1*$^{+}$) or three hotspots (in *tel1Δ*) near the middle of chromosome 3. DSB1 (in *ade6*) is ~16 kb from DSB2 (in *ura4A*) and ~45 kb from DSB3 (in *tel1::kanMX6*). (**A**) Scheme for determining DSB frequency at three hotspots (1, 2, and 3) near the middle of chromosome 3 by Southern blot hybridization of DNA cut by a restriction enzyme Z. See

Figure S3 for further explanation. (**B**) Strains GP8908 (*pat1-114 tel1*$^{+}$) and GP8907 (*pat1-114 tel1Δ*) were induced by raising the temperature to 34°C. DNA was extracted at the indicated times, digested with *Pme*I (which cuts at bp 1263677 and 1337886 in wt), and analyzed by Southern blot hybridization using a 0.75 kb radioactive probe near the middle of the 74.2 kb fragment (uncut; 66.3 kb in *tel1Δ*). (**C**) Quantification of the bands shows that the observed doubly-cut fragment (red bars) is less frequent than expected from independent breakage at the two hotspots (black bars) in wild type but more frequent than expected in *tel1Δ*. Note that the *tel1::kanMX6* mutation, about 45 kb to the left of the *ade6-3049* DSB hotspot, in strains GP8907 and GP8910 introduces a strong DSB hotspot, characteristic of such *kanMX6* insertions (23), giving rise to DSB3. (**D**) Analysis as in panel B but with strains GP8909 (*pat1-as1 tel1*$^{+}$) and GP8910 (*pat1-as1 tel1Δ*) induced at 34°C with the adenine analog 3-MB-PP1 (15). (**E**) Analysis as in panel C of expected and observed double-cut fragments shown in panel D.

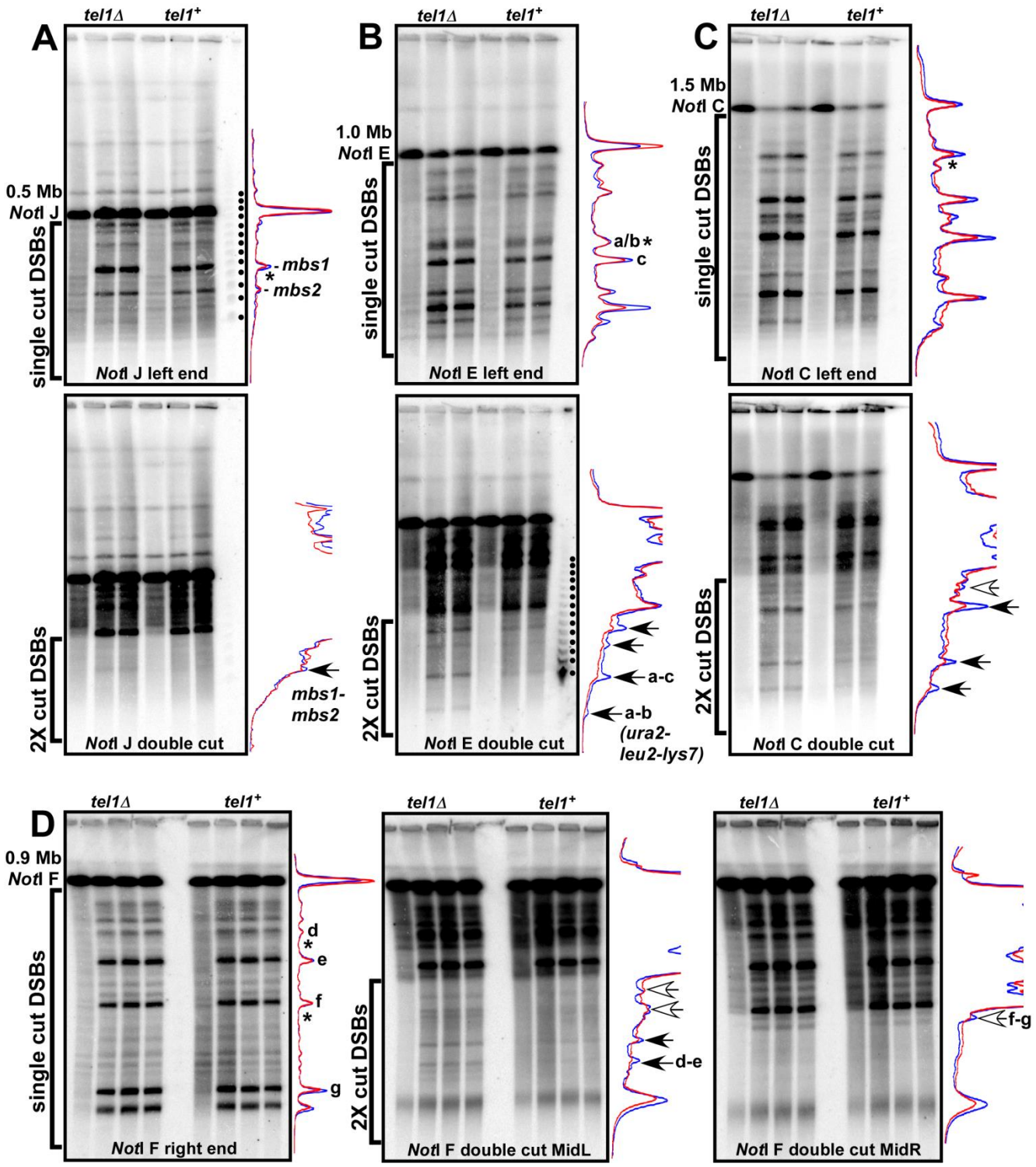

Figure S5. Interference of DSB formation at nearby hotspots depends on Tel1 DNA damage-response protein kinase: Analysis of DSBs at hotspots on *Not*I fragments on chromosomes 1 and 2. Shown are Southern blots with a probe from an end (for single cuts) or from the middle (for double cuts) of each fragment in *tel1Δ* (left three lanes) or in *tel1*$^{+}$ (right three lanes). Each set of three lanes

analyzes DNA from *pat1-114* cells harvested at 0, 5, and 6 hr after meiotic induction at 34°C; panel D has an additional time point at 4 hr. Lane traces to the right of each Southern blot are for *tel1Δ* (blue trace) or *tel1*$^{+}$ (red trace). Phage lambda DNA markers (concatemers of 48.5 kb) are visible in panel A (top) and panel B (bottom). **(A)** Distribution of DSBs across the 0.50 Mb *Not*I fragment J near the left end of chromosome 1 (top), and double-cut fragments generated from two meiotic DSBs, visualized by probing between *mbs1* and *mbs2* (bottom). **(B)** Distribution of DSBs across the 1.0 Mb *Not*I fragment E near the middle of chromosome 1 (top), and fragments generated from dual DSBs, visualized by probing between *ura2* and *leu2* (bottom, arrow a-b). **(C)** Distribution of DSBs across the 1.5 Mb *Not*I fragment C near the right end of chromosome 2, and fragments generated from dual DSBs, visualized by a probe at the position indicated (*). **(D)** Distribution of DSBs across the 0.90 Mb *Not*I fragment F near the middle of chromosome 1 (left); MidL (middle) and MidR (right) are separate middle-fragment probes between different pairs of DSB hotspots. The position of all respective double-cut probes are indicated by " ***** " on the DSB lane traces. Note that single-cut fragments are nearly equally frequent in *tel1Δ* and *tel1*$^{+}$ at some hotspots but are more frequent in *tel1Δ* at other hotspots (Table S1). Nevertheless, double-cut fragments are more prominent in *tel1Δ* than in *tel1*$^{+}$ for distances less than about 200 kb (black arrows); longer double-cut fragments are less dependent on Tel1 (white arrows). Quantification of labeled double-cut fragments is in Table S1. Double-cut fragments not labeled were not quantified because of multiple double-cut fragments of similar size, or uncertainty of DSB frequencies.

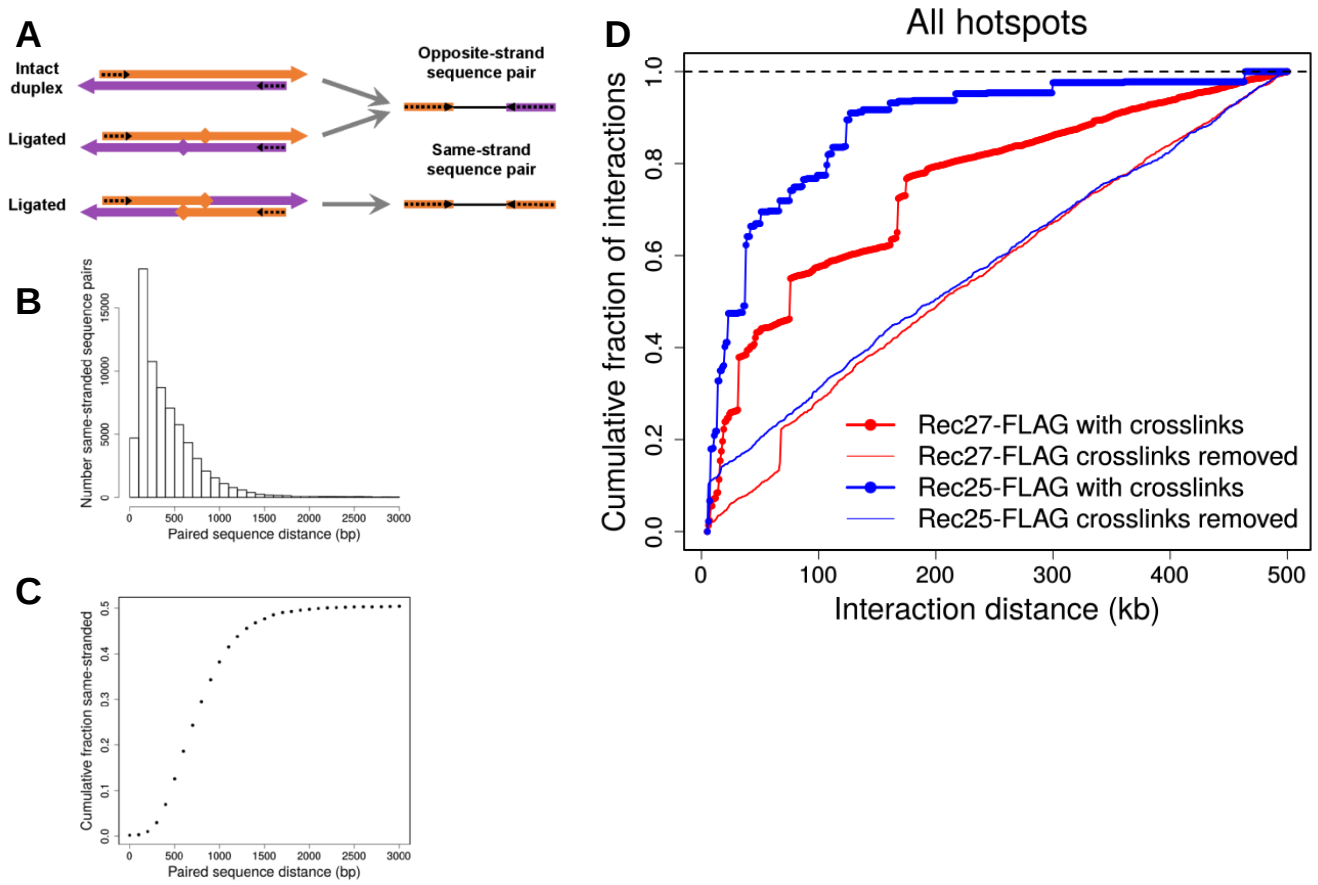

Figure S6. **Analysis of DNA in DSB hotspot clusters.** *Left*: DNA was sheared by sonication to <2 kb and analyzed by high-throughput 3C with IP. **(A)** Ligation of the two ends of one DNA molecule (intra-molecular ligation) gives rise to sequence pairs, from paired-end sequencing, on opposite strands, as do intact, non-ligated DNA molecules. Half of the inter-molecular ligations also give rise to sequence reads on opposite strands, and the other half to reads on the same strand. **(B)** Same-strand reads are highly enriched for short (<2 kb; mode, 100 – 200 bp) distances between reads but with a broad distribution. **(C)** Same-strand reads approach 50% of all reads as the distance between sequence pairs approaches 2 kb, the cutoff used here to ensure sequences were derived from inter-molecular ligations and thus interaction between DSB hotspots. *Right:* Physical clustering of DSB hotspots is limited to an ~200 kb chromosomal region. **(D)** DSB hotspot clustering was analyzed as in Figure 4F but with Rec27-FLAG (red lines) or Rec25-FLAG (blue lines) in place of Rec27-GFP, analyzed in Figures 4 and S1. Data are the summation of ligations between all genomic hotspots with chromatin crosslinks maintained before ligation (lines with data points) or with crosslinks removed just before ligation (lines without data points).

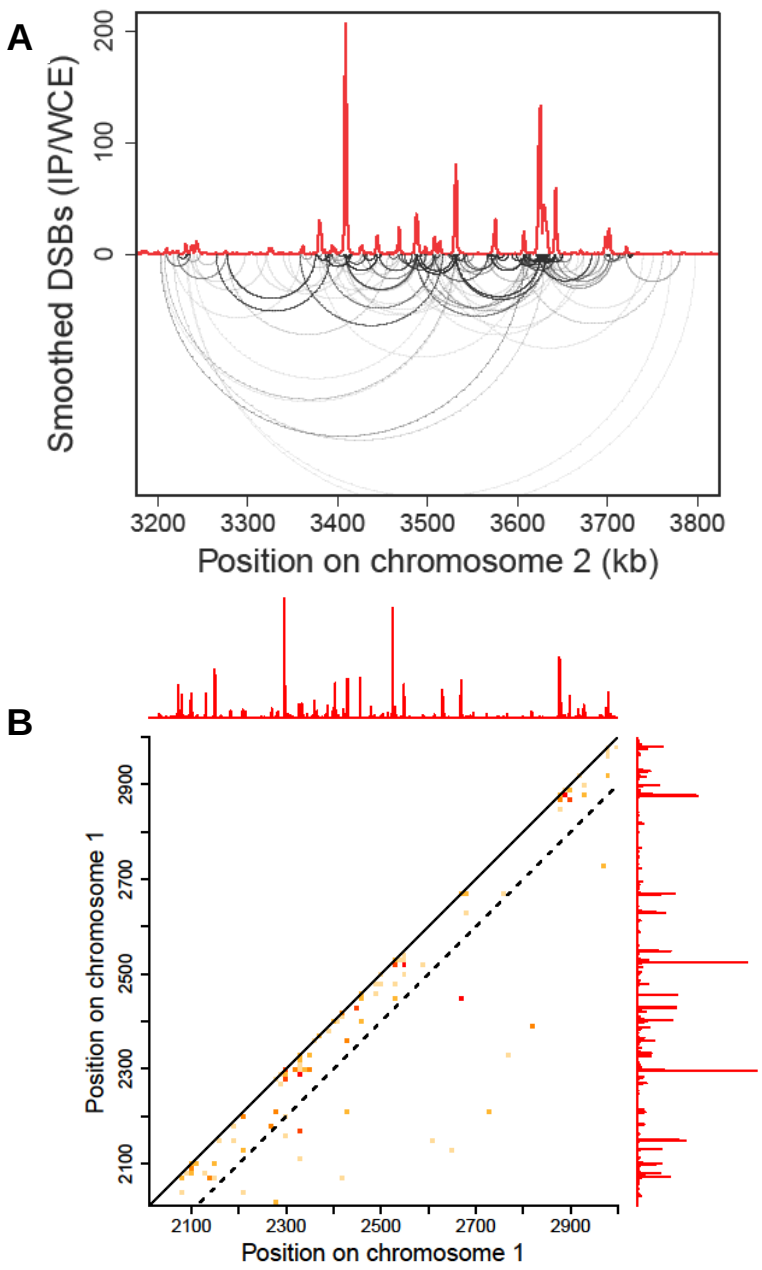

Figure S7. **(A) Analysis of DNA bound by Rec27-GFP**, which binds DSB hotspots with high specificity (1), shows preferential ligation of one hotspot DNA to another hotspot <~100 kb away (lower arcs; frequency indicated by darkness). **(B)** Standard contact heat-map of ligations (hot-hot and hot-cold) across part of chromosome 1. Frequency of ligations (number per kb) is scaled as in Figure 4C. DSB frequency relative to genome median (red line, on a linear scale) is from (6). Note that the map is sparsely populated due to the immunoprecipitation of chromatin and preferential ligations between specific loci (DSB hotspots), and that the greatest density of high-frequency ligations is within about 100 kb (dashed line).

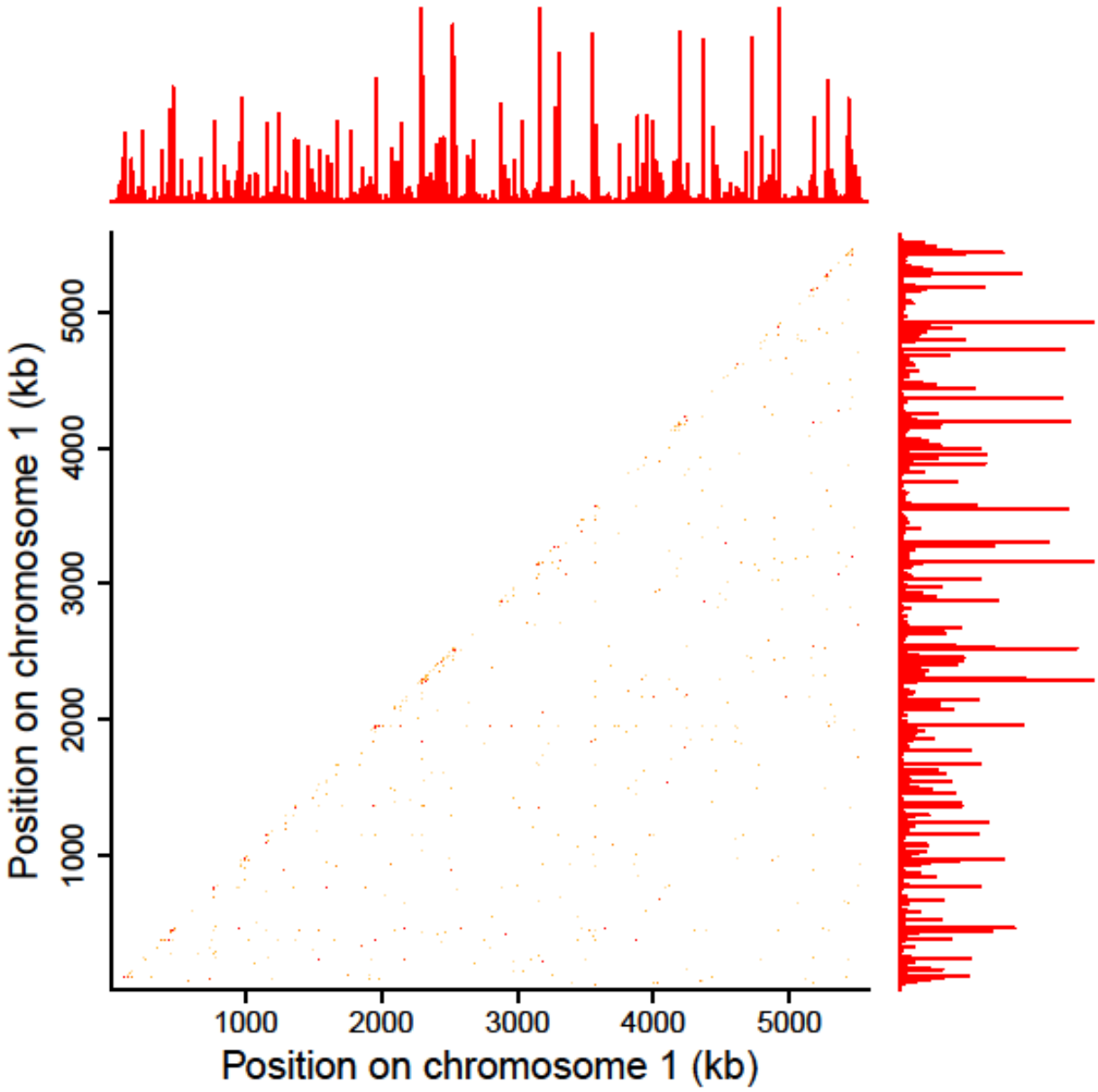

Figure S8. **Standard contact heat-map of ligations (hot-hot and hot-cold) across chromosome 1.** Frequency of ligations (number per kb) is scaled as in Figure 4C. DSB frequency relative to genome median (red line, on a linear scale) is from (6). Note that the map is sparsely populated due to the immunoprecipitation of chromatin and preferential ligations between specific loci (DSB hotspots), and that the greatest density of high-frequency ligations is within about 100 kb.

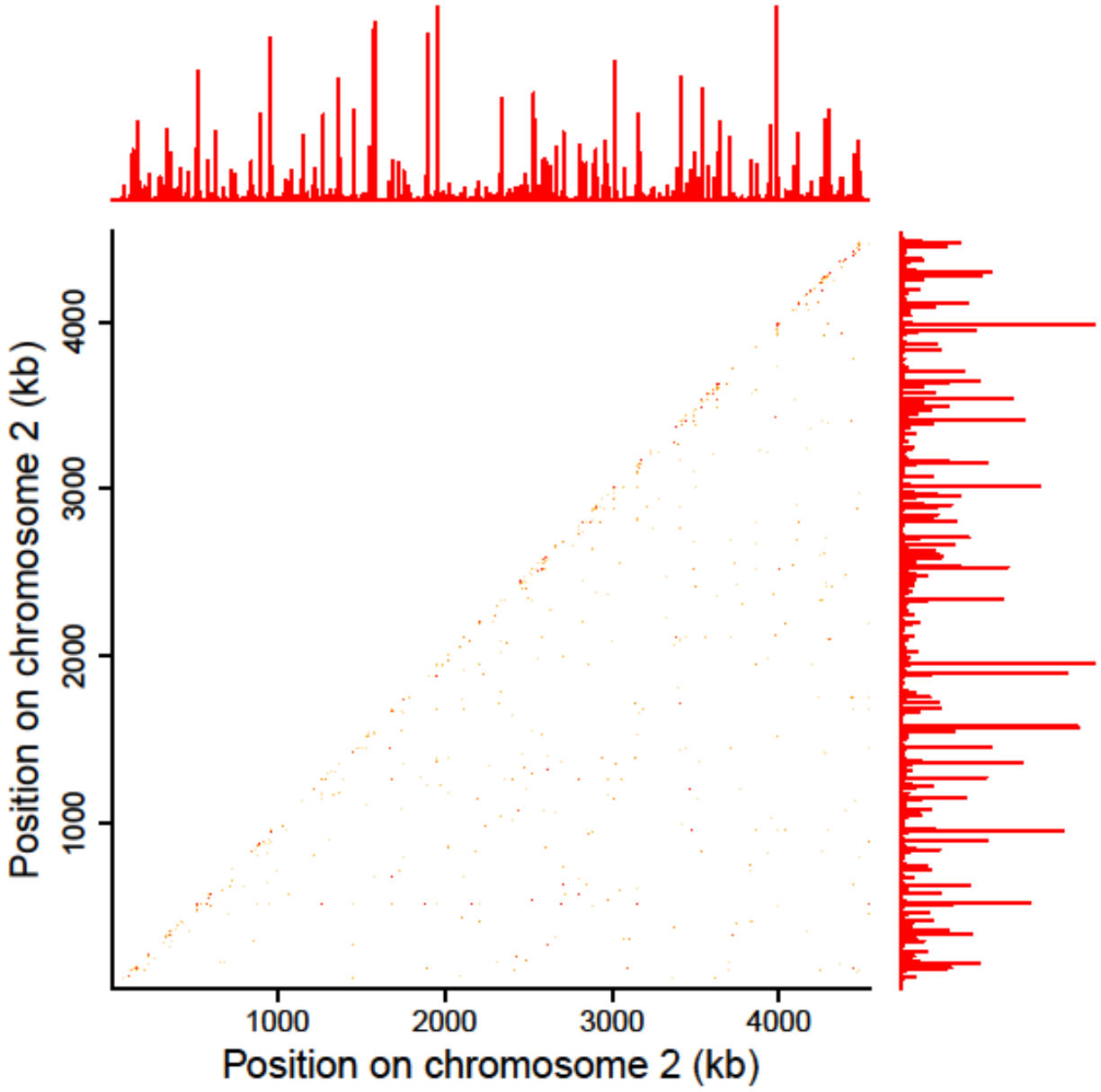

Figure S9. **Standard contact heat-map of ligations (hot-hot and hot-cold) across chromosome 2.** Frequency of ligations (number per kb) is scaled as in Figure 4C. DSB frequency relative to genome median (red line, on a linear scale) is from (6). Note that the map is sparsely populated due to the immunoprecipitation of chromatin and preferential ligations between specific loci (DSB hotspots), and that the greatest density of high-frequency ligations is within about 100 kb.

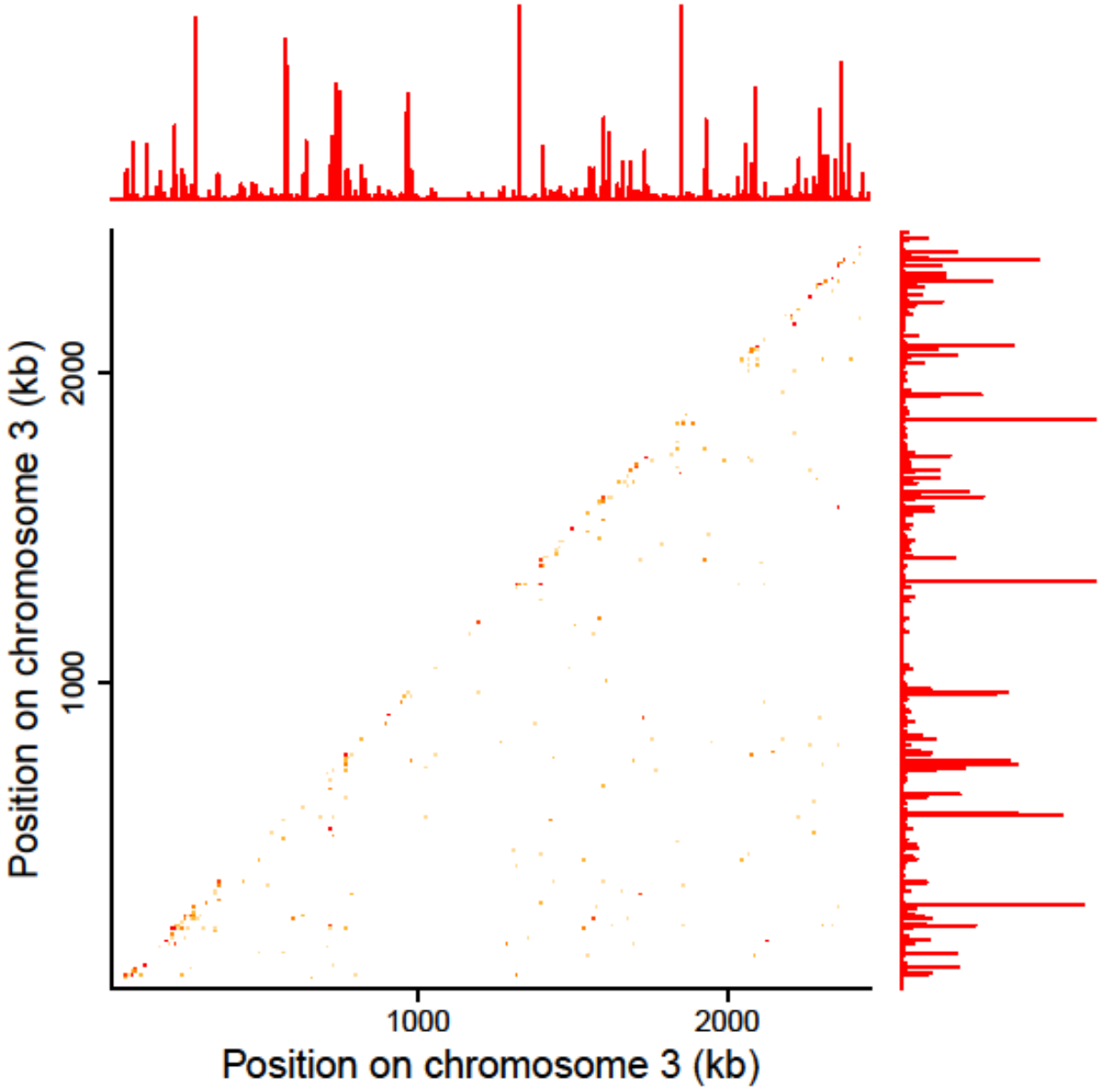

Figure S10. Standard contact heat-map of ligations (hot-hot and hot-cold) across chromosome 3. Frequency of ligations (number per kb) is scaled as in Figure 4C. DSB frequency relative to genome median (red line, on a linear scale) is from (6). Note that the map is sparsely populated due to the immunoprecipitation of chromatin and preferential ligations between specific loci (DSB hotspots), and that the greatest density of high-frequency ligations is within about 100 kb.

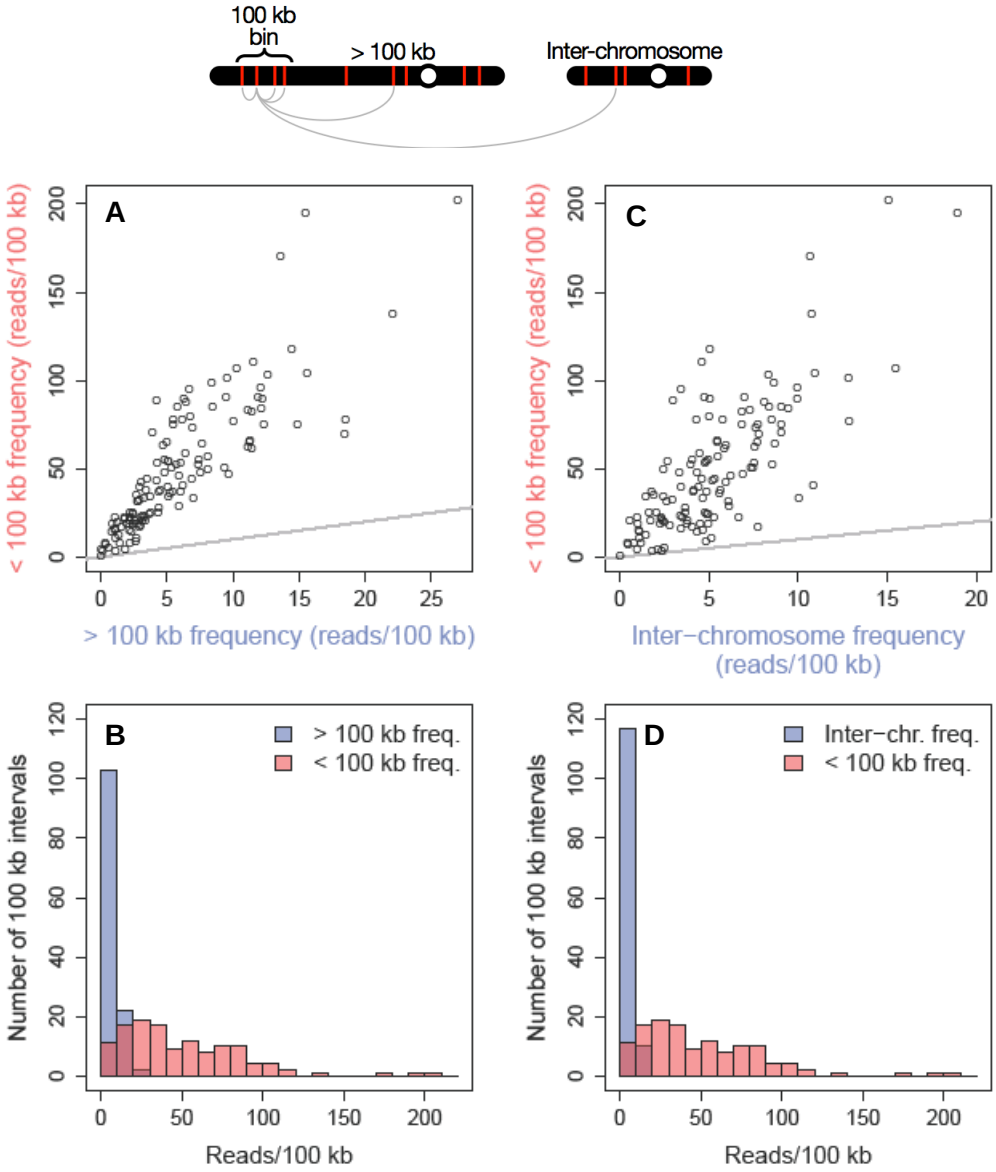

Figure S11. Non-specific ligations between hotspot DNA cannot account for the preferential interactions between hotspots less than 100 kb apart. (A) The genome was divided into 100 kb non-overlapping regions. For each region, sequence read-pairs were compiled if at least one end was in a hotspot within the region and the other in a hotspot on the same chromosome (left part of diagram at top of figure). For each region the number of read-pairs between this region and hotspots >100 kb away was divided by the amount of DNA in hotspots outside this region; similarly, the number of read-pairs between this region and hotspots <100 kb away was divided by the amount of hotspot DNA within this region. These normalized counts were then plotted against one another, with each point representing a 100 kb genomic region. The straight line indicates equality. **(B)** A histogram of the normalized values in panel A. **(C)** As in panel A, but instead compiling sequence read-pairs

between hotspots in each 100 kb region and hotspots on any another chromosome (right part of diagram at top of figure). For each region, the number of read-pairs was divided by the amount of DNA in hotspots on the other chromosomes. This was plotted against the frequency of read-pairs between hotspots <100 kb, as in panel A. **(D)** A histogram of the normalized values used in panel C.

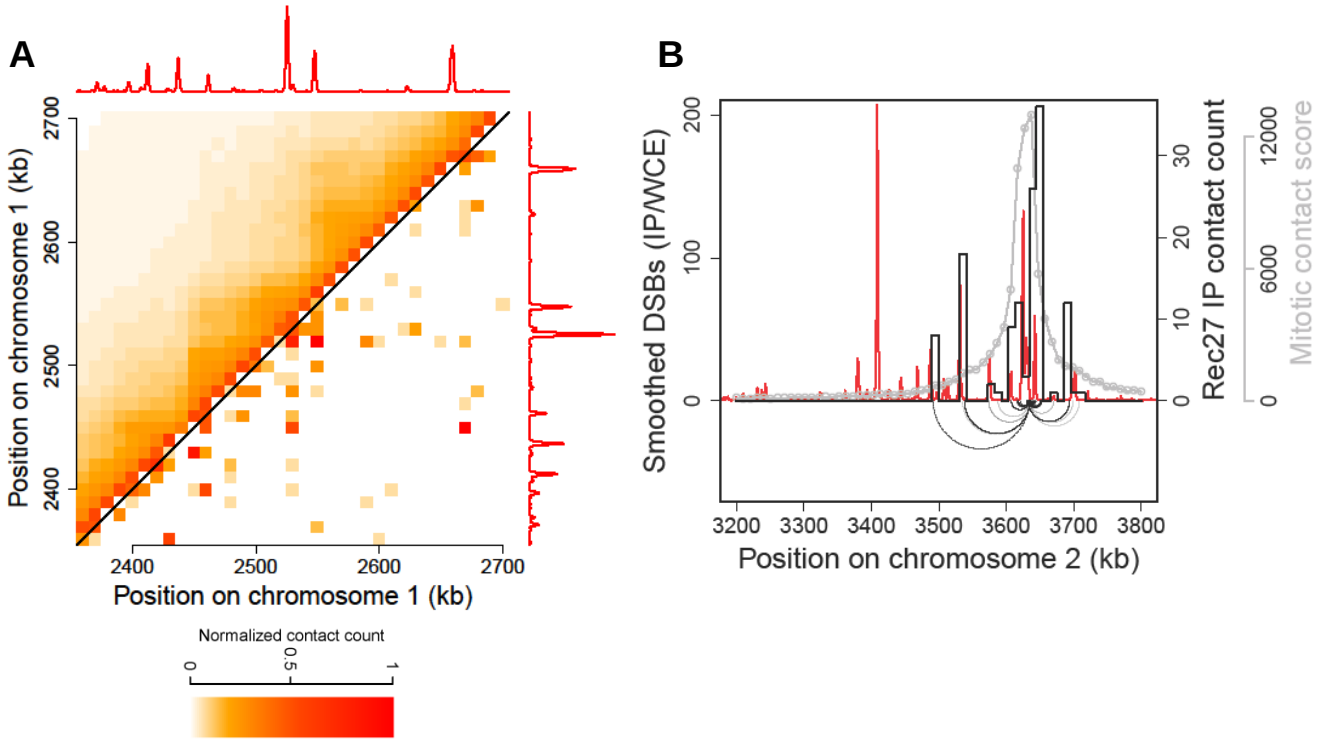

Figure S12. DSB hotspot-hotspot ligations are discontinuous, unlike continuous Hi-C ligations. (A) In this representative genomic interval, Hi-C signals (top left part of panel; ref. 29) indicate domains in which each chromosomal point contacts any other point with a frequency that decreases monotonically with distance, shown by the progressively decreasing darkness of the points indicating 10 kb bins. In sharp contrast, LinE cluster signals (bottom right part of panel) are discontinuous, reflecting preferential ligations between DSB hotspots (indicated by DSB frequency in the graphs above and to the right of the panel) (1). **(B)** The frequency of contacts decreases monotonically with distance in the Hi-C analysis (grey curve) but has multiple peaks in the LinE cluster analysis (bar graph summation of ligations shown by the arcs under DSB hotspots; Figure 4), indicating that DSB hotspots cluster preferentially within chromosomal domains. The similarity of the sizes of domains from the Hi-C data and the sizes of clusters may reflect formation of domains and clusters being influenced by related factors.

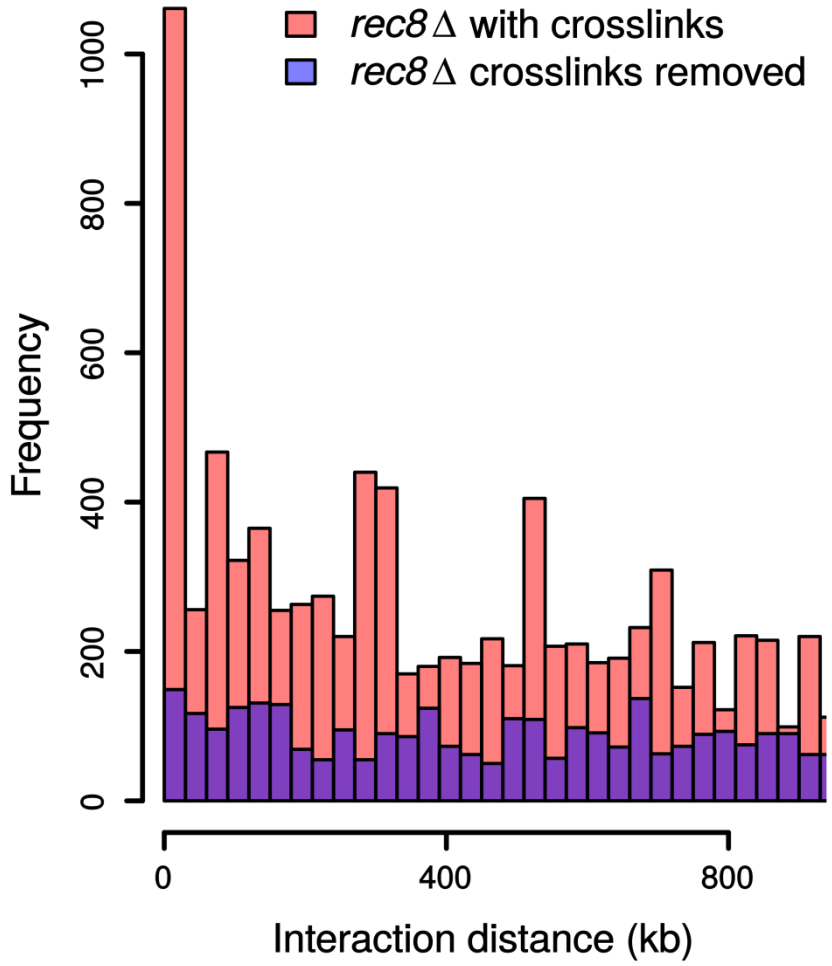

Figure S13. Hotspot interactions are farther apart in the absence of cohesin subunit Rec8. Strain GP8663 (*rec8::kanMX*) was analyzed as in Figure 4E; cumulative curves are in Figure 4F. Data are the frequency of ligations between pairs of sites located the indicated distance apart (in 30 kb bins) among all genomic hotspots with chromatin crosslinks maintained until after ligation (red bars) or with crosslinks removed just before ligation (purple bars).

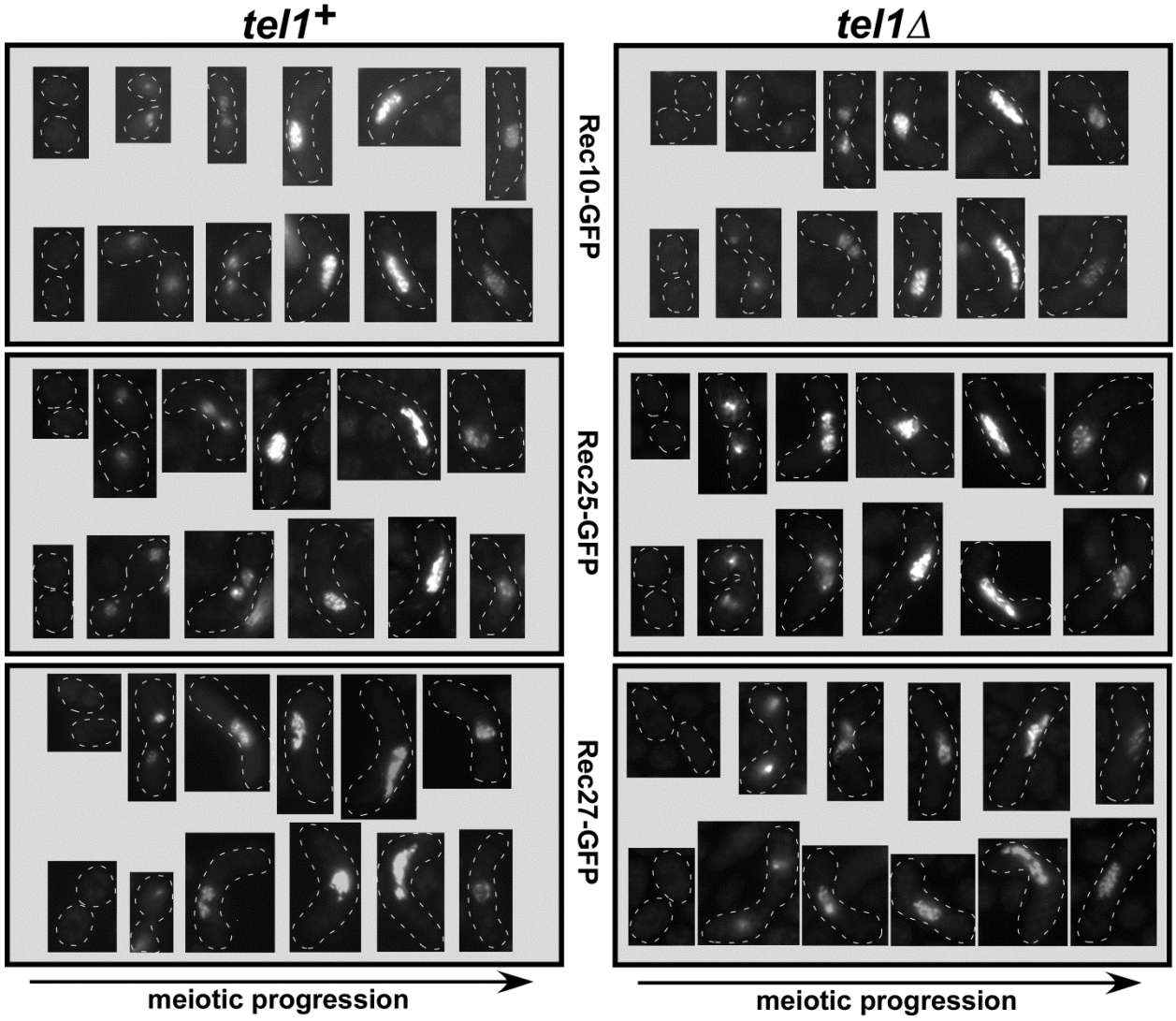

Figure S14. Tel1 DNA damage-response protein kinase is not required for formation of clustered foci of linear element (LinE) proteins Rec10, Rec25, and Rec27. Homothallic (h^{90}) strains with the indicated GFP fusion were spotted on MEA, incubated ~16 hr, and examined by fluorescence microscopy. Images from different cells at various stages of meiosis, in one microscopic field, were arranged in apparent temporal order (left to right). Two such reconstructions are shown for each strain. The stages represented are mating, karyogamy, horsetail movement, and initiation of MI, which occurred at similar frequencies in all strains. Dotted lines indicate the outline of each cell.